The effects of oleylethanolamide on feeding behavior involve hypothalamic oxytocin neurons

A Dissertation in Fullfilment of the Requirements for the Degree of Doctor of Philosophy in Toxicology

by

Pasqua Dipasquale

Department of Physiology and Pharmacology
Sapienza University of Rome

13 January 2009

Thesis Advisor:
Prof. Vincenzo Cuomo

Thesis Committee:
Prof. Maria Broccardo
Prof. Luigia Trabace
Prof. Maria Luisa Barbaccia

CONTENTS

CHAPTER I

GENERAL INTRODUCTION

ANANDAMIDE AND ITS ANALOGUE, OLEOYLETHANOLAMIDE:

In December 1992 Devane and his collaborators (Devane *et al.,* 1992) reported the isolation and structure elucidation of a porcine brain lipid component that selectively displaced the binding of a high-affinity cannabinoid receptor ligand to brain membrane preparations. This compound was the ethanolamide of arachidonic acid (20:4, n-6) and was named anandamide (AEA) (Figure 1), after the Sanskrit word for "bliss", ananda. AEA was shown to be active in the tetrade of mouse behavioral tests suggestive of cannabinoid-like activity, i.e. inhibition of locomotor and rearing activity, hypothermy, catalepsy, and analgesia (Fride and Mechoulam, 1993; Crawley *et al.,* 1993). Another derivative of arachidonic acid that activates cannabinoid receptors, 2-arachidonoylglycerol (2-AG), was discovered in 1995 (Mechoulam *et al.,* 1995; Sugiura *et al.,* 1995). Although structurally different from plant-derived cannabinoids, these compounds, in analogy with the "endorphins" (i.e. the endogenous ligands of opiate receptors), were named "endocannabinoids".

Additional natural fatty acid ethanolamides (FAEs) have been detected in virtually all mammalian cells, tissues and certain body fluids (Bachur *et al.,* 1965; Na-

tarajan *et al.,* 1985). They have also been identified in fish, invertebrates (Bisogno *et al.,* 1997; Sepe *et al.,* 1998), plants (Chapman *et al.,* 2000) and some microorganisms (Clarke *et al.,* 1976; Ellingson, 1980). In most mammalian cells and tissues FAEs consist primarly of saturated and monounsaturated species, such as palmitoylethanolamide (PEA), oleoylethanolamide (OEA), and stearoylethanolamide (SEA) (Figure 1). AEA is generally a minor component of cellular FAEs, with some exceptions, such as in the periimplantation mouse uterus (Schmid *et al.,* 1997).

It has been shown that FAEs are synthesized in response to a variety of physiological and pathological stimuli, including activation of neurotransmitter receptors in rat brain neurons (Di Marzo *et al.,* 1994; Giuffrida *et al.,* 1999), and exposure to metabolic stressors in mouse epidermal cells (Berdyshev *et al.,* 2000). That animal cells release FAEs in a stimuls-dependent manner suggests that these compounds may participate in cell-to-cell communication. Further support for this idea came from the discovery that AEA serves as an endogenous ligand for cannabinoid receptors. PEA, OEA and SEA cannot be considered endocannabinoids, since they have very low affinity for the cannabinoid receptors. Research on FAEs mediated signaling has been largely confined to the endocannabinoid AEA, however it is now becoming apparent that the cannabinoid receptor-inactive, saturated and monounsaturated FAEs are of physiological and patho-

logical interest as well.

HOW IS OEA SYNTHESIZED?

A model for OEA biosynthesis is illustrated schematically in Figure 2. Its first step is the transfer of a fatty acid residue from the *sn*-1 position of phosphatidylcholine to the free amine group of phosphatidylethanolamine. This reaction is catalyzed by an *N*-acyltransferase, which remains to be molecularly identified, and yields a heterogeneous family of *N*-acyl phosphatidylethanolamine (NAPE) species. The second step is the cleavage of NAPEs to produce other fatty acid ethanolamides (FAEs), including OEA, a step catalyzed by NAPE-specific phospholipaseD (NAPE-PLD) (Okamoto *et al*., 2004).

HOW IS OEA INACTIVATED?

Once released, polyunsaturated FAEs are transported back into cells (Beltramo *et al*., 1997; Cravatt *et al*., 1996; Désarnaud *et al*., 1995) and eventually broken down to fatty acid and ethanolamine by an intracellular fatty acid amide hydrolase (FAAH) (Figure 3) and/or *N*-acylethanolamine-hydrolyzing acid amidase (NAAA), a lysosomal cysteine hydrolase (Tsuboi *et al*., 2005).

It has been shown that AEA transport meets four key criteria of a carrier-mediated process: saturability, fast rate, temperature-dependence, and substrate

selectivity (Di Marzo *et al*., 1994 ; Beltramo *et al*., 1997; Hillard *et al*., 1997).

AEA transport differs from that of amine and amino acid transmitters in that it does not require cellular energy or external Na^+, implying that it may be mediated through facilitated diffusion (Beltramo *et al*., 1997; Hillard *et al*., 1997; Piomelli *et al*., 1999; Rakhshan *et al*., 2000). As far as OEA is concerned it is not clear yet if a specific transporter is responsible for its uptake into the cells.

FAAH (previously called 'anandamide amidohydrolase' and 'oleamide hydrolase') is an intracellular membrane-bound protein whose primary structure displays significant homology with the 'amidase signature family' of enzymes (Cravatt *et al*., 1996; Giang and Cravatt, 1997). It acts as a hydrolytic enzyme for fatty acid ethanolamides such as AEA, but also for esters such as 2-AG (Goparaju *et al*., 1998, Lang *et al*., 1999) and primary amides such as oleamide (Cravatt *et al*., 1995). Site-directed mutagenesis experiments indicate that this unusually wide substrate preference may be due to a novel catalytic mechanism involving the amino acid residue lysine 142. This residue may act as a general acid catalyst, favoring the protonation and consequent detachment of reaction products from the enzyme's active site (Patricelli *et al*., 1999). Three serine residues that are conserved in all amidase signature enzymes (S241, S217 and S218 in FAAH) may also be essential for enzymatic activity: serine 241 may serve as the enzyme's

catalytic nucleophile, while serine 217 and 218 may modulate catalysis (Patricelli *et al*., 1999).

OEA BIOLOGICAL ROLE

Although FAEs were first described four decades ago (Colodzin *et al*., 1963), they did not attract much attention until the discovery that AEA is an endogenous ligand for cannabinoid receptors, G protein-coupled receptors targeted by the marijuana constituent delta-9-tetrahydrocannabinol (THC) (Devane *et al*., 1992). AEA is now established as a brain endocannabinoid messenger (Piomelli, 2003) and multiple roles for other FAE have also been proposed (Mazzari *et al*., 1996; Calignano *et al*., 1998; Rodriguez de Fonseca *et al*., 2001). One emerging function of these lipid mediators is the regulation of feeding behavior. AEA causes overeating in rats because of its ability to activate cannabinoid receptors (Berry *et al*., 2002). This action is of therapeutic relevance: cannabinoid agonists such as THC are currently used to alleviate anorexia and nausea in AIDS patients, whereas the CB1 antagonist rimonabant (SR141716A) was recently found to be effective in the treatment of obesity (Berry *et al*., 2002).

In contrast to AEA, OEA decreases food intake and body weight gain through a cannabinoid receptor-independent mechanism (Fu *et al*., 2003; Guzman *et al*., 2004; Lo Verme *et al*., 2005). Despite its similarities with AEA, OEA does not

bind, indeed, to cannabinoid receptors and its functional roles have remained elusive for many years, until it was demonstrated that OEA may serve as physiological regulator of satiety and energy balance (Rodriguez de Fonseca *et al.,* 2001; Gaetani *et al.,* 2003; Oveisi *et al.,* 2004; Nielsen *et al.,* 2004). In the rat proximal small intestine, endogenous OEA levels decrease during fasting and increase upon refeeding, likely as a result of local alterations in OEA biosynthesis and/or hydrolysis (Rodriguez de Fonseca *et al.,* 2001). Dietary fat intake represents the main stimulus for OEA synthesis in enterocytes (Schwartz *et al.,* 2008). These periprandial fluctuations in OEA mobilization may represent a previously undescribed signal that modulates between-meal satiety. Pharmacological studies have shown, indeed, that, when administered as a drug, OEA produces profound anorexiant effects in rats and mice (Rodriguez de Fonseca *et al.,* 2001; Nielsen *et al.,* 2004; Proulx *et al.,* 2005), which are due to selective prolongation of feeding latency and post meal interval (Rodriguez de Fonseca *et al.,* 2001; Oveisi *et al.,* 2004). The behavioral selectivity of OEA is further underscored by the fact that this lipid amide does not induce visceral malaise, anxiety-like behaviors or stress hormone release (Rodriguez de Fonseca *et al.,* 2001; Proulx *et al.,* 2005).

OEA PHARMACOLOGICAL TARGET

The nuclear receptor peroxisome proliferator-activated receptor-(PPAR-alpha)

Figure 4 is a key regulator of lipid metabolism and energy balance in mammals (Desvergne *et al.,* 1999). Although OEA may bind to multiple receptors (Wang *et al.,* 2005; Overton *et al.,* 2006), three distinct lines of evidence indicate that PPAR-alpha mediates the satiety-inducing effects of this compound. Firstly, OEA binds with high affinity to the purified ligand-binding domain of mouse and human PPAR-alpha (K_D 37 and 40 nM, respectively) and activates with high potency PPAR-alpha-driven transactivation in a heterologous expression system EC_{50} = 120 nM (Fu *et al.,* 2003). Secondly, synthetic PPAR-alpha agonists, such as the compounds GW7647 and Wy-14643, exert anorexiant effects that are due to a selective increase in feeding latency and, thus, are behaviorally identical to those produced by OEA (Fu *et al.,* 2003). Thirdly, mutant mice in which the PPAR-alpha gene has been deleted by homologous recombination (PPAR-alpha$^{-/-}$ mice) do not respond to OEA or synthetic PPAR-alpha agonists, although they retain normal responses to two mechanistically different anorexiants, CCK-octapeptide (CCK-8) and fenfluramine (Fu *et al.,* 2003). Together, the findings outlined above suggest that endogenous OEA, produced in the proximal small intestine during feeding, regulates between-meal satiety by activating PPAR-alpha.

Although PPAR-alpha receptor are expressed also in the CNS, some evidences suggest that the anorexiant effect of OEA is mainly peripheral, rather than attributable to direct activation of central PPAR-alpha. In fact, OEA does not affect

food intake when injected into the brain ventricles, and its anorexic actions are prevented when peripheral sensory fibers are removed (Rodriguez de Fonseca *et al.,* 2001; Fu *et al.,* 2003). Moreover, both sistemic and oral administration of the compound cause a sustained decrease of food intake in free-feeding rats, which is accompanied by an increase in OEA levels in the gastrointestinal tract and in plasma, but not in the brain (Oveisi *et al.,* 2004).

Since the anorexiant effect of OEA appears to be selective and, in particular, not related to malaise and nausea, the question arises of which, if any, are the central nervous system (CNS) structures recruited downstream to OEA peripheral receptor activation and that are responsible for the behavioral effects of this lipid on feeding.

REFERENCES

Bachur, N. R., Masek, K., Melmon, K. L., and Udenfriend, S. (1965). "Fatty Acid Amides of Ethanolamine in Mammalian Tissues." J Biol Chem, 240, 1019-24.

Beltramo, M., Stella, N., Calignano, A., Lin, S. Y., Makriyannis, A., and Piomelli, D. (1997). "Functional role of high-affinity anandamide transport, as revealed by selective inhibition." Science, 277(5329), 1094-7.

Berdyshev, E. V., Schmid, P. C., Dong, Z., and Schmid, H. H. (2000). "Stress-induced generation of N-acylethanolamines in mouse epidermal JB6 P+ cells." Biochem J, 346 Pt 2, 369-74.

Berry, E. M., and Mechoulam, R. (2002). "Tetrahydrocannabinol and endocannabinoids in feeding and appetite." Pharmacol Ther, 95(2), 185-90.

Bisogno, T., Ventriglia, M., Milone, A., Mosca, M., Cimino, G., and Di Marzo, V. (1997). "Occurrence and metabolism of anandamide and related acylethanolamides in ovaries of the sea urchin Paracentrotus lividus." Biochim Biophys Acta, 1345(3), 338-48.

Calignano, A., La Rana, G., Giuffrida, A., and Piomelli, D. (1998). "Control of pain initiation by endogenous cannabinoids." Nature, 394(6690), 277-81.

Chapman, K. D. (2000). "Emerging physiological roles for N-acylphosphatidylethanolamine metabolism in plants: signal transduction and membrane protection." Chem Phys Lipids, 108(1-2), 221-9.

Clarke, N. G., Hazlewood, G. P., and Dawson, R. M. (1976). "Novel lipids of Butyrivibrio spp." Chem Phys Lipids, 17(2-3 SPEC NO), 222-32.

Colodzin, M., Bachur, N. R., Weissbach, H., and Udenfriend, S. (1963). "Enzymatic formation of fatty acid amides of ethanolamine by rat liver microsomes." Biochem Biophys Res Commun, 10, 165-70.

Cravatt, B. F., Giang, D. K., Mayfield, S. P., Boger, D. L., Lerner, R. A., and Gilula, N. B. (1996). "Molecular characterization of an enzyme that degrades neuromodulatory fatty-acid amides." Nature, 384(6604), 83-7.

Cravatt, B. F., Prospero-Garcia, O., Siuzdak, G., Gilula, N. B., Henriksen, S. J., Boger, D. L., and Lerner, R. A. (1995). "Chemical characterization of a family of brain lipids that induce sleep." Science, 268(5216), 1506-9.

Crawley, J. N., Corwin, R. L., Robinson, J. K., Felder, C. C., Devane, W. A., and Axelrod, J. (1993). "Anandamide, an endogenous ligand of the cannabinoid receptor, induces hypomotility and hypothermia in vivo in rodents." Pharmacol Biochem Behav, 46(4), 967-72.

Desarnaud, F., Cadas, H., and Piomelli, D. (1995). "Anandamide amidohydrolase activity in rat brain microsomes. Identification and partial characterization." J Biol Chem, 270(11), 6030-5.

Desvergne, B., and Wahli, W. (1999). "Peroxisome proliferator-activated receptors: nuclear control of metabolism." Endocr Rev, 20(5), 649-88.

Devane, W. A., Hanus, L., Breuer, A., Pertwee, R. G., Stevenson, L. A., Griffin, G., Gibson, D., Mandelbaum, A., Etinger, A., and Mechoulam, R. (1992). "Isolation and structure of a brain constituent that binds to the cannabinoid receptor." Science, 258(5090), 1946-9.

Di Marzo, V., Fontana, A., Cadas, H., Schinelli, S., Cimino, G., Schwartz, J. C., and Piomelli, D. (1994). "Formation and inactivation of endogenous cannabinoid anandamide in central neurons." Nature, 372(6507), 686-91.

Ellingson, J. S. (1980). "Identification of N-acylethanolamine phosphoglycerides and acylphosphatidylglycerol as the phospholipids which disappear as Dictyostelium discoideum cells aggregate." Biochemistry, 19(26), 6176-82.

Fride, E., and Mechoulam, R. (1993). "Pharmacological activity of the cannabinoid receptor agonist, anandamide, a brain constituent." Eur J Pharmacol, 231(2), 313-4.

Fu, J., Gaetani, S., Oveisi, F., Lo Verme, J., Serrano, A., Rodriguez De Fonseca, F., Rosengarth, A., Luecke, H., Di Giacomo, B., Tarzia, G., and Piomelli, D. (2003). "Oleylethanolamide regulates feeding and body weight through activation of the nuclear receptor PPAR-alpha." Nature, 425(6953), 90-3.

Gaetani, S., Oveisi, F., and Piomelli, D. (2003). "Modulation of meal pattern in the rat by the anorexic lipid mediator oleoylethanolamide." Neuropsychopharmacology, 28(7), 1311-6.

Giang, D. K., and Cravatt, B. F. (1997). "Molecular characterization of human and mouse fatty acid amide hydrolases." Proc Natl Acad Sci U S A, 94(6), 2238-42.

Giuffrida, A., Parsons, L. H., Kerr, T. M., Rodriguez de Fonseca, F., Navarro, M., and Piomelli, D. (1999). "Dopamine activation of endogenous cannabinoid signaling in dorsal striatum." Nat Neurosci, 2(4), 358-63.

Goparaju, S. K., Ueda, N., Yamaguchi, H., and Yamamoto, S. (1998). "Anandamide amidohydrolase reacting with 2-arachidonoylglycerol, another cannabinoid receptor ligand." FEBS Lett, 422(1), 69-73.

Guzman, M., Lo Verme, J., Fu, J., Oveisi, F., Blazquez, C., and Piomelli, D. (2004). "Oleoylethanolamide stimulates lipolysis by activating the nuclear receptor peroxisome proliferator-activated receptor alpha (PPAR-alpha)." J Biol Chem, 279(27), 27849-54.

Hillard, C. J., Edgemond, W. S., Jarrahian, A., and Campbell, W. B. (1997). "Accumulation of N-arachidonoylethanolamine (anandamide) into cerebellar granule cells occurs via facilitated diffusion." J Neurochem, 69(2), 631-8.

Lang, W., Qin, C., Lin, S., Khanolkar, A. D., Goutopoulos, A., Fan, P., Abouzid, K., Meng, Z., Biegel, D., and Makriyannis, A. (1999). "Substrate Specificity and Stereoselectivity of Rat Brain Microsomal Anandamide Amidohydrolase." J Med Chem, 42(9), 1682.

Lo Verme, J., Gaetani, S., Fu, J., Oveisi, F., Burton, K., and Piomelli, D. (2005). "Regulation of food intake by oleoylethanolamide." Cell Mol Life Sci, 62(6), 708-16.

Mazzari, S., Canella, R., Petrelli, L., Marcolongo, G., and Leon, A. (1996). "N-(2-hydroxyethyl)hexadecanamide is orally active in reducing edema formation and inflammatory hyperalgesia by down-modulating mast cell activation." Eur J Pharmacol, 300(3), 227-36.

Mechoulam, R., Ben-Shabat, S., Hanus, L., Ligumsky, M., Kaminski, N. E., Schatz, A. R., Gopher, A., Almog, S., Martin, B. R., Compton, D. R., and et al. (1995). "Identification of an endogenous 2-monoglyceride, present in canine gut, that binds to cannabinoid receptors." Biochem Pharmacol, 50(1), 83-90.

Natarajan, V., Schmid, P. C., Reddy, P. V., Zuzarte-Augustin, M. L., and Schmid, H. H. (1985). "Occurrence of N-acylethanolamine phospholipids in fish brain and spinal cord." Biochim Biophys Acta, 835(3), 426-33.

Nielsen, M. J., Petersen, G., Astrup, A., and Hansen, H. S. (2004). "Food intake is inhibited by oral oleoylethanolamide." J Lipid Res, 45(6), 1027-9.

Okamoto, Y., Morishita, J., Tsuboi, K., Tonai, T., and Ueda, N. (2004). "Molecular characterization of a phospholipase D generating anandamide and its congeners." J Biol Chem, 279(7), 5298-305.

Oveisi, F., Gaetani, S., Eng, K. T., and Piomelli, D. (2004). "Oleoylethanolamide inhibits food intake in free-feeding rats after oral administration." Pharmacol Res, 49(5), 461-6.

Overton, H. A., Babbs, A. J., Doel, S. M., Fyfe, M. C., Gardner, L. S., Griffin, G., Jackson, H. C., Procter, M. J., Rasamison, C. M., Tang-Christensen, M., Widdowson, P. S., Williams, G. M., and Reynet, C. (2006). "Deorphanization of a G protein-coupled receptor for oleoylethanolamide and its use in the discovery of small-molecule hypophagic agents." Cell Metab, 3(3), 167-75.

Patricelli, M. P., Lovato, M. A., and Cravatt, B. F. (1999). "Chemical and mutagenic investigations of fatty acid amide hydrolase: evidence for a family of

serine hydrolases with distinct catalytic properties." Biochemistry, 38(31), 9804-12.

Piomelli, D. (2003). "The molecular logic of endocannabinoid signalling." Nat Rev Neurosci, 4(11), 873-84.

Piomelli, D., Beltramo, M., Glasnapp, S., Lin, S. Y., Goutopoulos, A., Xie, X. Q., and Makriyannis, A. (1999). "Structural determinants for recognition and translocation by the anandamide transporter." Proc Natl Acad Sci U S A, 96(10), 5802-7.

Proulx, K., Cota, D., Castaneda, T. R., Tschop, M. H., D'Alessio, D. A., Tso, P., Woods, S. C., and Seeley, R. J. (2005). "Mechanisms of oleoylethanolamide-induced changes in feeding behavior and motor activity." Am J Physiol Regul Integr Comp Physiol, 289(3), R729-37.

Rakhshan, F., Day, T. A., Blakely, R. D., and Barker, E. L. (2000). "Carrier-mediated uptake of the endogenous cannabinoid anandamide in RBL-2H3 cells." J Pharmacol Exp Ther, 292(3), 960-7.

Rodriguez de Fonseca, F., Navarro, M., Gomez, R., Escuredo, L., Nava, F., Fu, J., Murillo-Rodriguez, E., Giuffrida, A., LoVerme, J., Gaetani, S., Kathuria, S., Gall, C., and Piomelli, D. (2001). "An anorexic lipid mediator regulated by feeding." Nature, 414(6860), 209-12.

Schmid, P. C., Paria, B. C., Krebsbach, R. J., Schmid, H. H., and Dey, S. K. (1997). "Changes in anandamide levels in mouse uterus are associated with uterine receptivity for embryo implantation." Proc Natl Acad Sci U S A, 94(8), 4188-92.

Schwartz, G. J., Fu, J., Astarita, G., Li, X., Gaetani, S., Campolongo, P., Cuomo, V., and Piomelli, D. (2008). "The lipid messenger OEA links dietary fat intake to satiety." Cell Metab, 8(4), 281-8.

Sepe, N., De Petrocellis, L., Montanaro, F., Cimino, G., and Di Marzo, V. (1998). "Bioactive long chain N-acylethanolamines in five species of edible bivalve molluscs. Possible implications for mollusc physiology and sea food industry." Biochim Biophys Acta, 1389(2), 101-11.

Sugiura, T., Kondo, S., Sukagawa, A., Nakane, S., Shinoda, A., Itoh, K., Yamashita, A., and Waku, K. (1995). "2-Arachidonoylglycerol: a possible endogenous cannabinoid receptor ligand in brain." Biochem Biophys Res Commun, 215(1), 89-97.

Tsuboi, K., Sun, Y. X., Okamoto, Y., Araki, N., Tonai, T., and Ueda, N. (2005). "Molecular characterization of N-acylethanolamine-hydrolyzing acid amidase, a novel member of the choloylglycine hydrolase family with structural and functional similarity to acid ceramidase." J Biol Chem, 280(12), 11082-92.

Wang, X., Miyares, R. L., and Ahern, G. P. (2005). "Oleoylethanolamide excites vagal sensory neurones, induces visceral pain and reduces short-term food intake in mice via capsaicin receptor TRPV1." J Physiol, 564(Pt 2), 541-7.

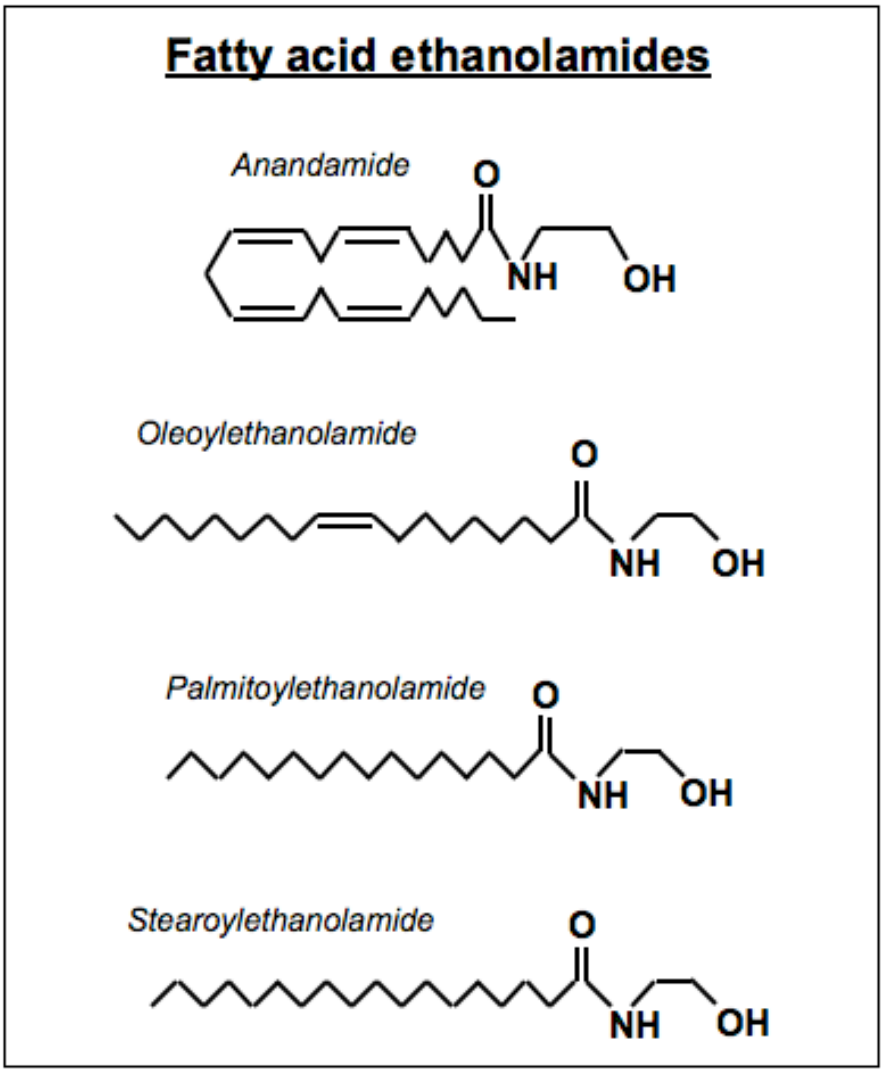

Figure 1. Anandamide and other fatty acid acyl ethanolamides

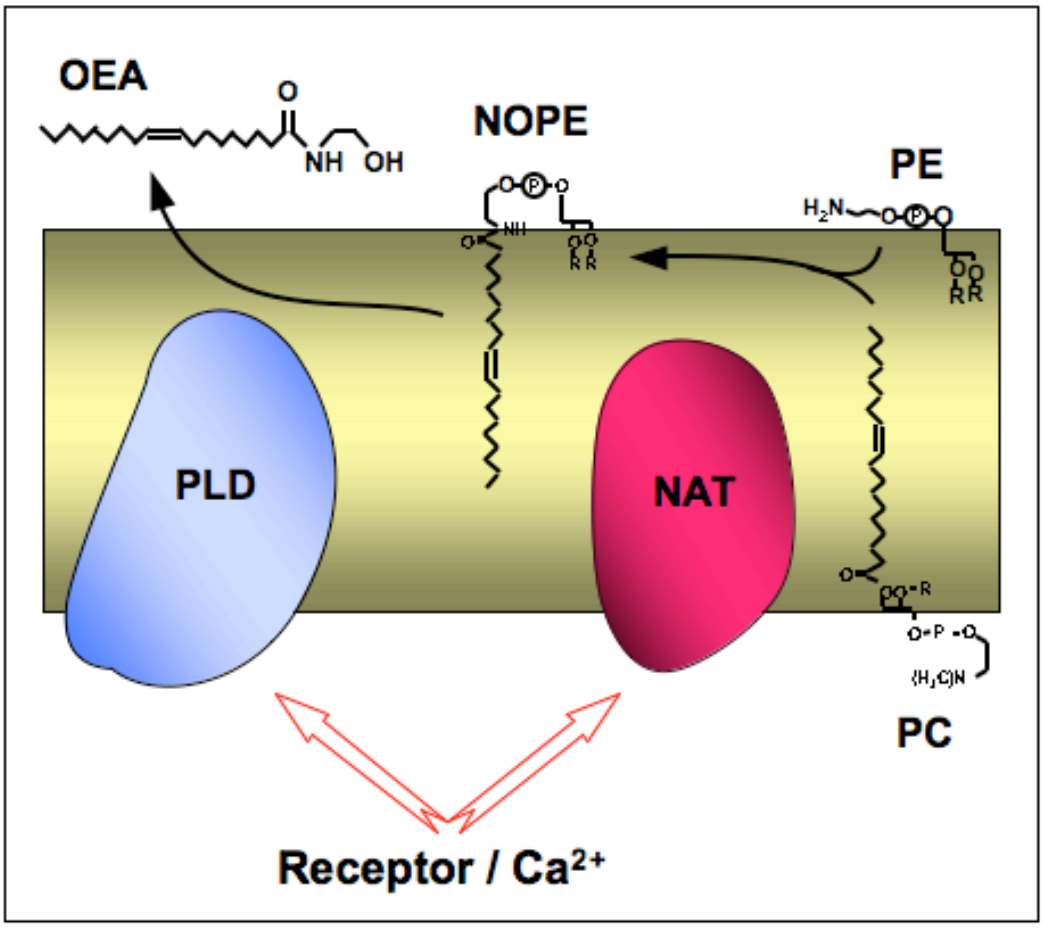

Figure 2. Model for OEA biosynthesis (see text).
NOPE=N-oleoylphosphatidylethanolamine;
PE=phosphatidylethanolammine;
PC=phosphatidylcholine;
PLD=phospholipase D;
NAT=N-acyltransferase

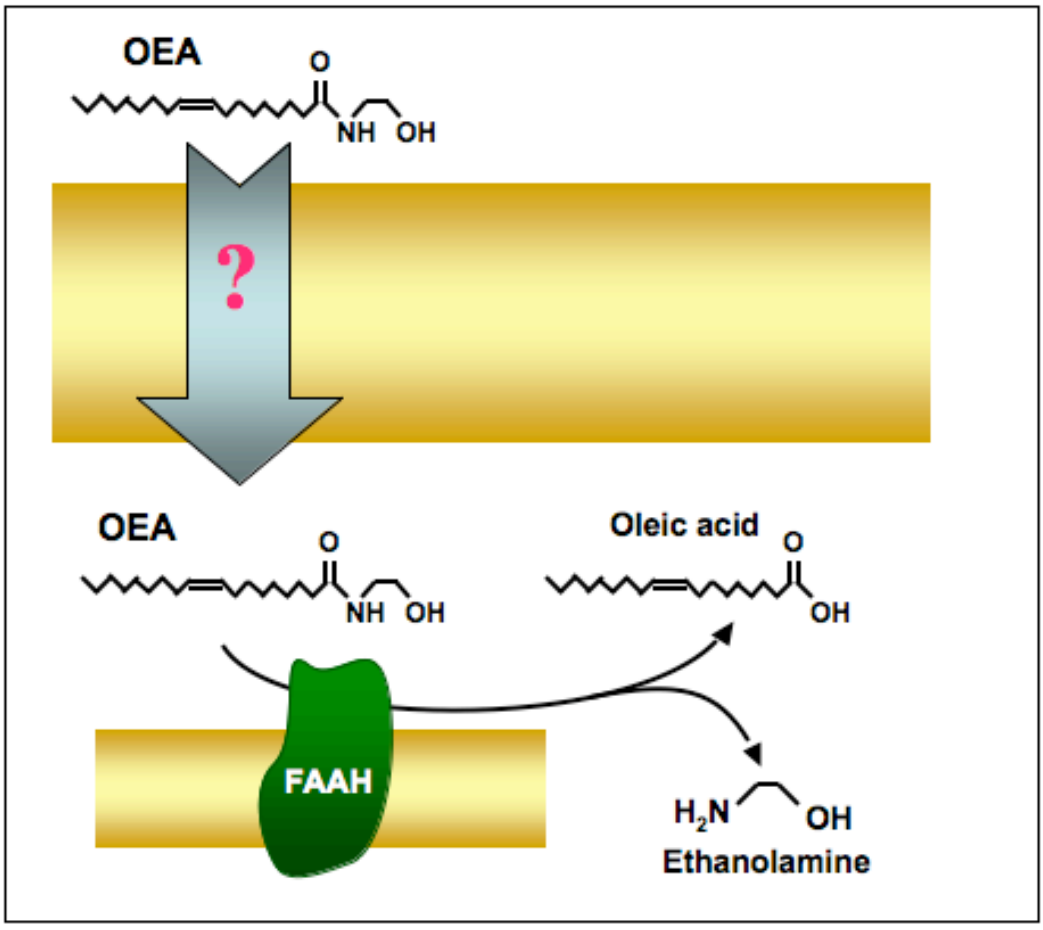

Figure 3. Model for OEA catabolism (see text).
FAAH=fatty acid amide hydrolase

CHAPTER II

STANDARDIZED ANALYSIS OF c-fos mRNA EXPRESSION PATTERN IN RAT BRAIN AUTORADIOGRAPHY USING FREEWARE IMAGING SOFTWARE:

INTRODUCTION:

The immediate early gene c-fos is one of the most studied genes in the CNS as a marker for neuronal activation (Edwards *et al.,* 1999; Abraham and Kovacs, 2000; Konkle and Bielajew, 2004). The c-fos belongs to the family of immediate-early transcription factor genes that are believed to function in coupling short-term signals to long-term changes in cellular phenotype by orchestrating changes in target gene expression (Curran and Morgan, 1995).

The expression of c-fos, which is normally low, can be increased by a number of pharmacological, physiological, and behavioral manipulations (Morgan and Curran, 1989; Herrera and Robertson, 1996). Therefore, the measurement of c-Fos protein levels, the product of c-fos gene, has been used as a marker for activated neurons (Hoffman *et al.,* 1993; Edwards *et al.,* 1999; Abraham and Kovacs,

2000). In recent years, c-Fos protein and c-fos mRNA have been widely used as markers for the impact of drug treatments (Young *et al.,* 1991; Kreuter *et al.,* 2004), experimental procedures (Worley *et al.,* 1993; Del Bel *et al.,* 1998), and environmental changes such as light (Rusak *et al.,* 1992), temperature (Bratincsak and Palkovits, 2004), and novelty/stress (Emmert and Herman, 1999; Amico *et al.,* 2004).

It is clear that c-fos gene expression is one of the most important CNS parameters in the field of neuroscience research. However, the traditional method of studying c-fos gene expression by examining c-Fos-positive neurons is a labor intensive task (Snowball *et al.,* 2000; Nakagawa *et al.,* 2003; Sinniger *et al.,* 2004). A more rapid way to analyze activated brain areas is to investigate the expression of c-fos mRNA by in situ hybridization with a radiolabeled probe that allows the detection of hybridized areas by autoradiography. However, c-fos mRNA expression is relatively low in basal conditions, therefore autoradiography of c-fos hybridized brain does not show a strong signal. As a consequence, the identification of brain areas activated after an experimental treatment can often be very difficult and usually relies upon the anatomical skills of the experimenter. The identification step is usually followed by the quantification procedure consisting of measuring the optical density of a sampling area of standard size for each hybridized brain region.

The aim of the study was to develop and validate a novel method for fast quantitative analysis of the optical density in the autoradiographic signal of hybridized slides.

METHODS

Animals and Experimental Conditions

Adult male Wistar rats were housed in groups of 6 rats per cage and kept at constant ambient temperature and humidity under a steady light/dark cycle with free access to food and water.

The day of the experiment the rats were divided in two experimental groups. In the first group, each rat was left undisturbed in its own cage and represented our control group; in the second group, each rat was individually transferred to an empty cage containing fresh sawdast, where it was kept for one hour, before being sacrificed and represented our treated group (called manipulated group). Rats were sacrificed with CO2 and decapitated. Their brains were rapidly excised, snap frozen in 2-methylbutane (-50°C) and stored at -80°C. Even though it takes several seconds for the animal to succumb after CO_2 inhalation, this method of sacrifice does not influence the level of expression of our gene of interest (Miller, 1991).

Tissue preparation

Brains were cut on a cryostat set at -20°C into four series of serial coronal sections at 20 μm thickness. Sections were thaw-mounted on Superfrost plus slides

(Menzel Glaser, Germany), three sections per slides, and immediately fixed in phosphate-buffered 4% paraformaldehyde for 1 hour. Sections were washed three times in 50 mM PBS, pH 7.4, for 10 min each before the slides were transferred for 10 min to 0.4% Triton X-100. The slides were rinsed in double distilled water (ddH_2O) and transferred to 0.1 M triethanolamine, pH 8.0. Acetic anhydride was added under stirring to a final concentration of 0.25% (v/v), and sections were further incubated for 10 min. The slides were rinsed twice in 50mM PBS, pH 7.4, for 10 min each before dehydration in 50 and 70% 2-propanol. The air-dried sections were stored at -20°C until the hybridization. Slides can be stored this way for several months with no apparent reduction in hybridization signal intensity.

In all these pre-hybridization steps common RNAse-free procedures were adopted to minimize degradation of mRNAs within the tissue sample and to ensure a strong hybridization signal.

Radiolabeled cRNA probe

Antisense c-fos riboprobe was transcribed from 1 μg *Pst* I-linearized recombinant clone pBS/rfos with T7 RNA polymerase in the presence of both uridine-5'-[α-^{35}S]thio]triphosphate and cytidine-5'-[α-^{35}S]thio]triphosphate. The resulting cRNA was complementary to positions 583-1250 of clone pc-fos(rat)-1 (Curran *et al*., 1987). The sense RNA sequence was generated from the same template using T3 RNA polymerase after linearization with *Pvu* II.

After transcription, the probes were subjected to mild alkaline hydrolysis as described previously (Angerer *et al.,* 1987) and purified on G-50 column (Bio-rad), according to the manufacturer's instructions.

Hybridization with radioprobes

The radioprobes were diluted in hybridization buffer (3X SSC, 50 mM NaPO4, 10 mM DTT, 1X Denhardt's solution, 20 mg/ml yeast tRNA, 10% dextran sulfate, and 50% formamide) to yield concentrations of 75,000 dpm/μl. Brain sections were coated with 55 μl of hybridization solution, slides were coverslipped and incubated for 16 h at 60°C in a humid chamber. Coverslips were removed, and slides were washed in 2X SSC and 1X SSC (20 min each), followed by incubation for 30 min at 37°C in RNase buffer (10 mM Tris, pH 8.0, 0.5 M NaCl, and 1 mM EDTA) containing 1 U/ml RNase T1 and 20 μg/ml RNase A, to reduce background. The slides were washed at room temperature in 1X and 0.2X SSC (20 min each), then under high stringency conditions at 60°C in 0.2X SSC (60 min), and at room temperature in 0.2X SSC (10 min). Finally, they were dehydrated in ascending alcohols series and air dried for about 2 hours.

Slides were exposed to Kodak Biomax film (Sigma Aldrich) for 3 days. The films were developed according to the manifacturer's protocol. Coexposure with two calibrated microscales (0.13-35.0 μCi/g and 4.47-400 μCi/g, respectively) of ^{14}C-labeled plastic standards (American Radiolabeled Chemicals Inc.) permitted

quantification of the ^{35}S radioisotope (Miller, 1991). The specificity of the hybridization signal was ascertained by hybridization of adjacent sections labeled with the correnspondingsense probe.

For emulsion autoradiography, selected sets of slides were dipped into NTB Kodak autoradiography emulsion (Integra Biosciences, Fernwald, Germany) and exposed for 18 days (c-fos hybridization) at 4°C. Autoradiograms were developed according to manifacturer's instructions. Finally slides were stained with cresyl violet staining. In particular, sections were incubated with warm 1% cresyl violet acetate (Sigma Aldrich) for 10 min. Stained slides were rinsed in ethanol, cleared in xylene, and coverslipped. Slices were examined in bright-field under a NIKON 80*i* ECLIPSE microscope.

Autoradigraphic quantitative analysis

Three different procedures were followed, being the first one our new procedure and the other two classic procedures that we used to validate the new protocol: 1) Whole area procedure; 2) Sampling area procedure; 3) Grain counting procedure.

Quantitative analysis of the autoradiographic film was performed using the freeware software from the National Institutes of Health (Scion Image software). Autoradiography films were first scanned (Epson perfection 3200 PHOTO) at high resolution (900 dpi). Resulting images were divided into single slice crops for quantification. Optical densities were converted into radioactivity concentra-

tions by densitometric analysis of ^{14}C-miscoscale standards that were used to create a calibration curve.

Whole area procedure

To analyze the optical density of the regions of interest (ROI) from each slice incubated with the antisense probe, a crop template was created from the brain tables illustrated on the "The Rat Brain Atlas" by Paxinos & Watson (1998). In particular, a proper plate was chosen that could correspond to the brain slice to analyze. Then, the pdf file from the atlas CD-ROM was transformed into a tiff file, calculating the proper pixel to mm ratio that reproduced the same resolution and the same size of the brain crop to analyze (Figure 1).

The tiff file containing the drawing from the atlas was opened with the IMAGE J software. The wand tool was used to create the selection of each ROI from the atlas template by simply clicking inside near the right edge, or outside to the left of the ROI on the template (Figure 2). The drawing of the atlas was then superimposed on the slice crop. All the ROIs created from the template were then applied to the new image containing the brain crop and the atlas drawing, and the optical density of each ROI was measured in one click (Figure 2). The template obtained from the atlas was also superimposed to the image of the Nissl stained slices taken with microscope.

Sampling area procedure

Initial quantification of c-fos mRNA hybridization signal was conducted on autoradiographs in sampled regions of the secondary motor cortex (M2) (Figure 3). This method was performed by arbitrarily circling an area on the region of interest and measuring its optical density with the calibration curve created with ^{14}C-miscoscale standards (Ferguson *et al*., 2004).

Grain counting procedure

Assessment of grain density over neurons of secondary motor cortex was performed by a semiautomated computerized grain-counting protocol. Images of lightly counterstained neurons of secondary motor cortex (M2) were captured at 2X in bright-field under a NIKON 80*i* ECLIPSE microscope (Figure 4). Square areas were manually sampled, and area determinations were made within Image Software. Images were then thresholde to visualize grains only, and area determinations were repeated. The sampling template was then moved to an unhybridized region of tissue to establish background grain area. Results were expressed as the percent of area occupied by grains (Bowers *et al*., 1998), calculated as:

$$\% \text{ area} = \frac{\text{(sampled area occupied by grains)} - \text{(background area occupied by grains)}}{\text{Total area of sampling template}} \times 100$$

RESULTS AND DISCUSSION

Analysis of c-fos hybridizated slices showed that the manipulation treatment evokes a significant increase in c-fos mRNA level in secondary motor cortex (M2). Here, we compared the induction of c-fos mRNA in brain of rats exposed to manipulation with three different method of quantification: whole area, sampling area, and grain counting procedure. The purpose of this experiment was to develop and validate a rapid way for quantification of the optical density of hybridized areas that does not involve either sampling or manually encircling the entire region of interest.

Results obtained from the analysis of optical density and of grain counting are reported in Figure 5. For each set of data we used a two-tailed t-test to compare data obtained from manipulated rats to data obtained from control rats.

The results shown in Figure 5 revealed that the accurancy of the anatomical reference from the atlas that was the basis of the whole area procedure improved the results of the statistical analysis with respect to both the sampling area method and the grain counting method.

The statistical analysis of the optical density measured with the sampling area procedure (Figure 5, panel B) gave the following results: $t= 30$; $df = 2$, $p < 0.01$

The t-test of the integrated optical density obtained with the whole area procedure gave the following results $t = 86,65$; $df = 2$, $p < 0.0001$

Finally, the statistical analysis of the percentage area of c-fos+ cells in the motor secondary gave the following results t-test: $t = 4.943$; $df = 2$ $p < 0.05$

This study illustrates a novel method to identify the brain areas hybridized with c-fos mRNA probe by using an unbiased template from "The Rat Brain Atlas" by Paxinos and Watson (1998). It describes a rapid way for quantification of the optical density of hybridized areas that does not involve either sampling or manually encircling the entire region of interest.

REFERENCES

Abraham, I. M., and Kovacs, K. J. (2000). "Postnatal handling alters the activation of stress-related neuronal circuitries." Eur J Neurosci, 12(8), 3003-14.

Angerer, L. M., Cox, K. H., and Angerer, R. C. (1987). "Demonstration of tissue-specific gene expression by in situ hybridization." Methods Enzymol, 152, 649-61.

Amico, J. A., Mantella, R. C., Vollmer, R. R., and Li, X. (2004). "Anxiety and stress responses in female oxytocin deficient mice." J Neuroendocrinol, 16(4), 319-24.

Bowers, G., Cullinan, W. E., and Herman, J. P. (1998). "Region-specific regulation of glutamic acid decarboxylase (GAD) mRNA expression in central stress circuits." J Neurosci, 18(15), 5938-47.

Bratincsak, A., and Palkovits, M. (2004). "Activation of brain areas in rat following warm and cold ambient exposure." Neuroscience, 127(2), 385-97.

Curran, T., Gordon, M. B., Rubino, K. L., and Sambucetti, L. C. (1987). "Isolation and characterization of the c-fos(rat) cDNA and analysis of post-translational modification in vitro." Oncogene, 2(1), 79-84.

Curran, T., and Morgan, J. I. (1995). "Fos: an immediate-early transcription factor in neurons." J Neurobiol, 26(3), 403-12.

Del Bel, A.A., Silveira, M.C.L., Graeff, F.G., Garcia-Cairasco, N., Guimaraes, F.S., (1998). " Differential expression of c-fos mRNA and Fos protein in the rat brain after restraint stress or pentylenetetrazole-induced seizures". Cell Mol Neurosci 18, 339–346.

Edwards, C.M., Abusnana, S., Sunter, D., Murphy, K.G., Ghatei, M.A., Bloom, S.R., (1999). "The effect of the orexins on food intake: comparison with neuropeptide Y, melanin-concentrating hormone and galanin". J. Endoocrinol 160, R7–R12.

Emmert, M.H., and Herman, J.P., (1999). " Differential forebrain c-fos mRNA induction by ether inhalation and novelty: evidence for distinctive stress pathways". Brain Res 845, 60–67

Ferguson, S.M., Thomas, M.J., Robinson, T.E., (2004). "Morphine-induced c-fos mRNA expression in striatofugal circuits: modulation by dose, environmental context, and drug history". Neuropsychopharmacology. 29, 1664-1674.

Herrera, D. G., and Robertson, H. A. (1996). "Activation of c-fos in the brain." Prog Neurobiol, 50(2-3), 83-107.

Hoffman, G.E., Smith, M.S., Verbalis, J.G., (1993). "C-Fos and related immediate early gene products as markers of activity in neuroendocrine systems". Front Neuroendocrinol 14, 173–213.

Konkle, A. T., and Bielajew, C. (2004). "Tracing the neuroanatomical profiles of reward pathways with markers of neuronal activation." Rev Neurosci, 15(6), 383-414.

Kreuter, J.D., Mattson, B.J., Wang, B., You, Z.B., Hope, B.T., (2004). "Cocaine-induced Fos expression in rat striatum is blocked by chloral hydrate or urethane". Neuroscience 127, 233–242.

Miller, J.A., (1991). "The calibration of ^{35}S or ^{32}P with ^{14}C-labeled brain paste or ^{14}C-plastic standards for quantitative autoradiography using LKB Ultrofilm or Amersham Hyperfilm". Neurosci. Lett. 121, 211–214

Morgan, J. I., and Curran, T. (1989). "Stimulus-transcription coupling in neurons: role of cellular immediate-early genes." Trends Neurosci, 12(11), 459-62.

Nakagawa, T., Katsuya, A., Tanimoto, S., Yamamoto, J., Yamauchi, Y., Minami, M., and Satoh, M. (2003). "Differential patterns of c-fos mRNA expression in the amygdaloid nuclei induced by chemical somatic and visceral noxious stimuli in rats". Neurosci Lett, 344(3), 197-200.

Rusak, B., McNaughton, L., Tobertyson, H.A., Hunt, S.P., (1992). "Circadian variation in photic regulation of immediate-early gene mRNA in rat suprachiasmatic nucleus cells". Mol Brain Res 14, 124–130.

Sinniger, V., Porcher, C., Mouchet, P., Juhem, A., Bonaz, B., (2004). "C-Fos and CRF receptor gene transcription in the brain of acetic acidinduced somato-visceral pain in rats". Pain 110, 738–750.

Snowball, R.K., Semmenenko, F.M., Lumb, B.M., (2000). "Visceral inputs to neurons in the anterior hypothalamus including those that project to the periaqueductal gray: a functional, anatomical and electrophysiological study". Neuroscience 99, 351–361.

Worley, P.F., Bhat, R.V., Baraban, J.M., Erickson, C.A., McNaughton, B.L., Barnes, C.A., (1993). "Thresholds for synaptic activation of transcription factors in hippocampus: correlation with long-term enhancement. J. Neuro-sci". 13, 4776–4786.

Young, S. T., Porrino, L. J., and Iadarola, M. J. (1991). "Cocaine induces striatal c-fos-immunoreactive proteins via dopaminergic D1 receptors." Proc Natl Acad Sci U S A, 88(4), 1291-5.

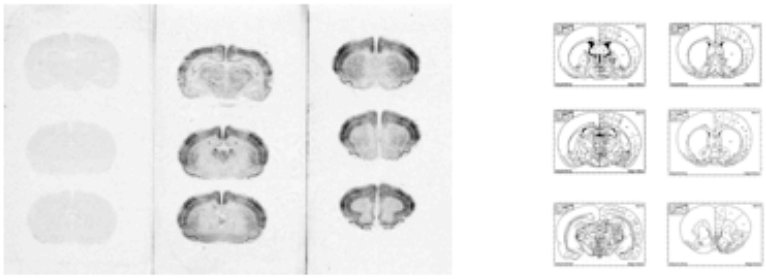

C-fos SENSE C-fos ANTISENSE

Figure 1. Hybridization of the sense and antisense c-fos probe and identification of a brain template from " The rat Brain Atlas" by Paxinos & Watson. Hybridization specificity was verified by the lack of any autoradiographic signal in the slices incubated with the sense probe of c-fos.

WHOLE AREA PROCEDURE

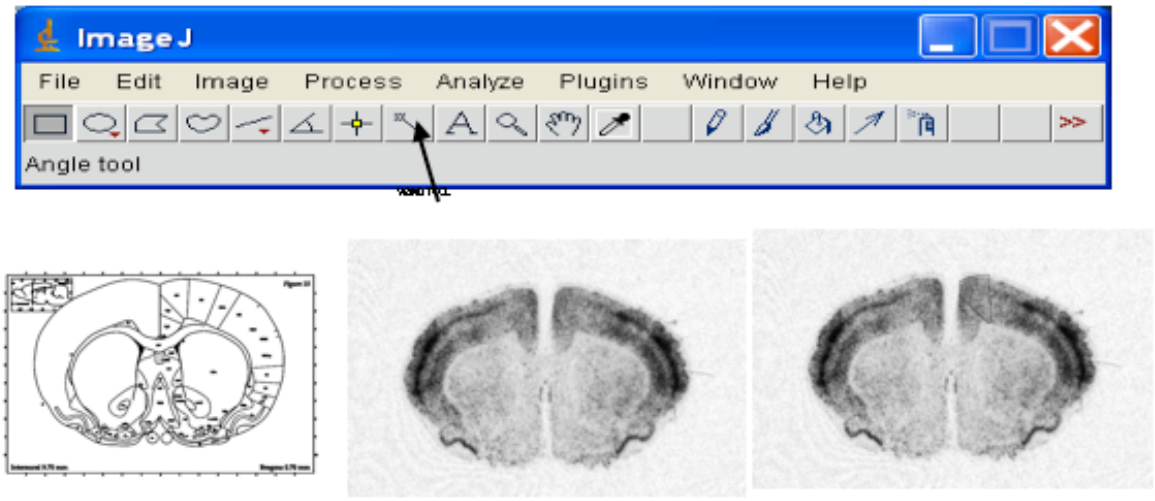

Figure 2. Analysis of ROI optical density of secondary motor cortex (M2). The drawing of the atlas was superimposed on the brain slice and quantified with calibration curve.

SAMPLING AREA PROCEDURE

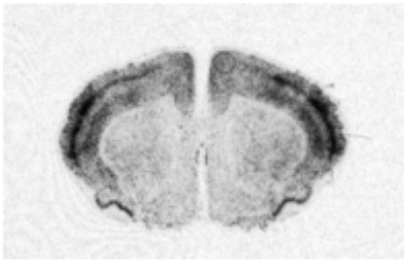

Figure 3. Representative autoradiography of a brain coronal section of a manipulated rat hybridized with c-fos riboprobe. The circle represents the sampling area of the secondary motor cortex (M2) in which the optical density was quantified .

GRAIN COUNTING PROCEDURE

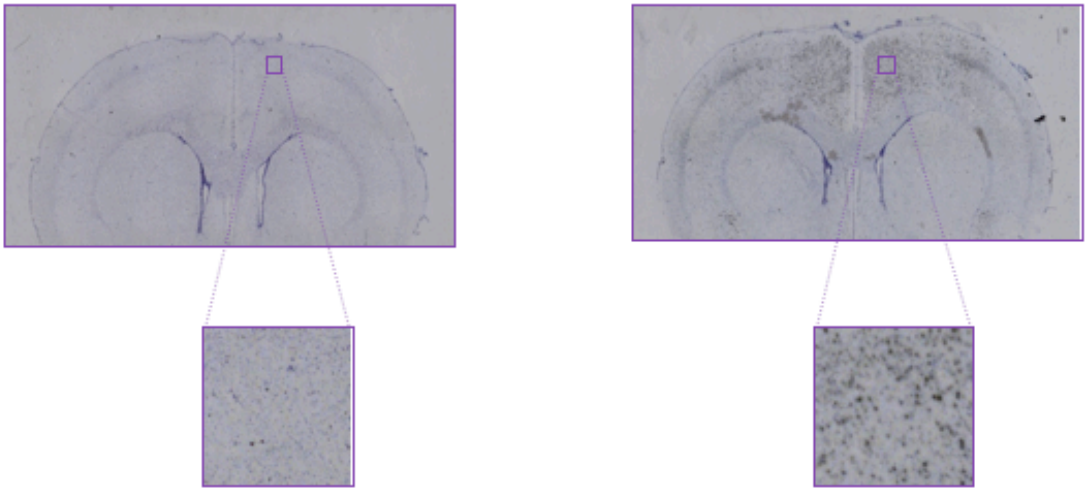

Figure 4. Illustration of emulsionate coronal section of control and manipulated rats. The box represents the area of secondary motor cortex (M2) where the number of hyridized c-fos cells was counted.

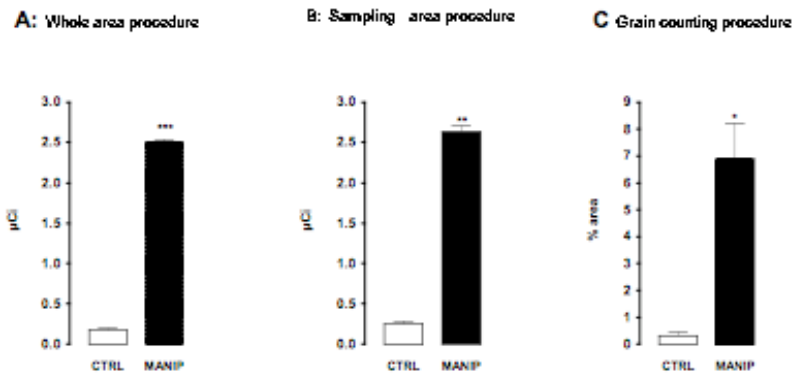

Figure 5. Quantitative analysis of c-fos mRNA in secondary motor cortex (M2) in control rats and manipulated rats obtained following three distimct procedures: whole area procedure (**A**), sampling area procedure (**B**), and grain counting procedure (**C**).
*p< 0.05; ***p< 0.01 ***p< 0.0001 vs respective control (t-test)

CHAPTER III

INVOLVEMENT OF CENTRAL NEUROPEPTIDERGIC PATHWAYS IN THE ANOREXIC EFFECT OF OLEOYLETHANOLAMIDE

INTRODUCTION:

Initial data obtained mapping mRNA levels for the activity regulated gene c-*fos* by *in situ* hybridization showed that, after systemic administration, OEA evokes a highly localized increase in c-*fos* mRNA levels in the nucleus of the solitary tract (NTS), the paraventricular nucleus (PVN) and the sopraoptic nucleus (SO) (Rodriguez de Fonseca *et al*., 2001).

These areas are crucially involved in the regulation of feeding behavior and energy balance and the stimulation of c-*fos* expression at these levels after intraperitoneal injection of OEA is consistent with the role of this compound as a peripheral regulator of satiety.

The NTS is the site where vagal afferents from the gastrointestinal tract predominantly terminate, together with sensory fibres from gustatory receptors and visceral fibres from the cardiovascular and respiratory systems. NTS neurons are activated after feeding, gut distension, intragastric infusion of nutrients or peripheral CCK administration.

Most of the NTS neurons that are activated by CCK or feeding project to the hypothalamus, including PVN and SO (Hillebrand *et al.,* 2002; Moore and Black 1991).

The PV and the SO nuclei are both part of the supraoptic region of the hypothalamus. The PVN consists of several distinct cell groups that define the dorsal, the ventral and the medial parvocellular sub-nuclei, and the lateral magnocellular subnucleus. The SO nucleus consists mainly of large neurons. The magnocellular components of both nuclei release two hormones, namely oxytocin (oxy) and vasopressin (avp). Increasing evidence suggests that the involvement of oxy and avp in a number of homeostatic systems may include appetite control (Hillebrand *et al.,* 2002).

The magnocellular oxy neurons of the SON and PVN project their axons to the posterior pituitary where they secrete oxy into the periphery. These neurons also release very large amounts of oxy from their dendrites and cell bodies within the SON and PVN. Dendritic oxy acts locally to facilitate neuron activity, but is also

thought to diffuse to distant sites within the brain; for example, the amygdale (Ludwig and Leng, 2006). Parvocellular oxy neurons of the PVN project centrally to various hypothalamic, limbic and brainstem regions. In particular, it has been reported that these neurons project to the NTS and that this neuronal pathway is related to inhibition of food intake (Blevins *et al.,* 2004; Sabatier *et al.,* 2006).

So central oxytocin systems can provide a multi-level controlling influence on other brain regions and, there is growing appreciation that oxy has an important role in the regulatory neuronal network mediating satiety (Amico *et al.,* 2005; Rinaman *et al.,* 2005; Mantella *et al.,* 2004).Based on these evidence, we hypothesized that oxy neurons, might play a key role in regulating food intake after OEA administration.

We explored such hypothesis by using two complementary approaches: anatomical/functional and pharmacological/behavioral. First we determined the effects of OEA (10 mg kg^{-1} i.p.) administration on the expression of oxy and avp mRNA in both PVN and SON by using in situ hybridization histochemistry. In particular, we performed a time-course study, to assess the time-dependent effects of OEA and its possible specificity toward one of the two neuropeptides. Second, we administered OEA at different doses (5, 10 and 20 mg kg^{-1}, i.p.), and sacrificed rats at the time that corresponded to the strongest effect, in order to determine the dose-dependent effects of OEA. Third, we determined if OEA causes any altera-

tion on oxy mRNA expression in the same neurons expressing c-fos. In this case we performed a dual in situ hybridization in brain slices obtained from rats treated with OEA at the most effective dose and time. Finally, we investigated whether the effects observed after OEA administration can be still detected in mice lacking the molecular target of the compound, namely the PPAR-alpha receptors.

The role of oxy in mediating OEA effects was further investigated by pharmacological/behavioral experiments, in which the systemically effective oxy antagonist, Atosiban (ATO, 1 mg kg^{-1} i.p.), was administered prior to OEA treatment, to evaluate its effects on preventing OEA-induced anorexia.

METHODS

Animals and experimental conditions

Adult male Wistar rats (Harlan, Italy) 250-300 g male PPAR-$\alpha^{-/-}$ mice (B6.129S4-*Ppara*^{tmt}GonzN12), and wild-type controls (C57/Bl6) (Germantown, NY) were housed in groups of three-four in standard plexiglas cages at a room temperature of 22°C. A 12 h light/dark cycle was set with the light on at 6:30 pm. Water and standard chow pellets were available ad libitum.

For in situ hybridization experiments, we accustomed rats to handling and injection procedures for 7 days. On day 8, we administered vehicle or OEA about 10 minutes before the dark phase of the light cycle and killed rats with CO2 and decapitation 30 min**,** 1, 2 and 4 hours after treatment. Both a dose-response experiments and a time-course experiment were performed. Mice were treated at the same time of the light/dark cycle and were sacrificed 1 hour after treatment. The brains were rapidly excised, snap frozen in 2-methylbutane (-50°C) and stored at -80°C.

For behavioral experiments rats were moved to individual cages two days prior to test with food pellets and water available ad libitum. On test day they were treated before dark onset and left undisturbed for 18 hours.

All procedures met the guidelines from the Italian Ministry of Health as well as from the US National Institutes of Health for the care and use of laboratory animals.

Treatments

OEA was synthesized in the laboratory (Giuffrida *et al.,* 2000), dissolved in saline/polyethylene glycol/Tween 80 (90/5/5, v/v/v; 2 ml Kg^{-1}) and administered, 10 min before dark onset, by intraperitoneal (i.p.) injection at dose of 5, 10 or 20 mg Kg^{-1} to free-feeding rats (FFO). Control animals (FFV) received an i.p. injection of vehicle. OEA was administered also to free-feeding wild type and PPAR-$\alpha^{-/-}$ mice (W-type O and K-out O, respectively) at the dose of 10 mg Kg^{-1}. Control mice (W-type V and K-out V, respectively) received injection of vehicle.

The oxy receptor antagonist atosiban (ATO) 1mg kg^{-1} was dissolved in saline and administered to rats 30 min before OEA or vehicle administration. Control animals received a saline injection instead of ATO

Tissue preparation

Brains were cut on a cryostat set at -20°C into four series of serial coronal sections at 20 μm thickness. Sections were thaw-mounted on Superfrost plus slides (Menzel Glaser, Germany), three sections per slides in the case of rat sections or four sections per slides in the case of mouse sections, and immediately fixed in phosphate-buffered 4% paraformaldehyde for 1 hour. Sections were washed three

times in 50 mM PBS, pH 7.4, for 10 min each before the slides were transferred for 10 min to 0.4% Triton X-100. The slides were rinsed in double distilled water (ddH_2O) and transferred to 0.1 M triethanolamine, pH 8.0. Acetic anhydride was added under stirring to a final concentration of 0.25% (v/v), and sections were further incubated for 10 min. The slides were rinsed twice in 50mM PBS, pH 7.4, for 10 min each before dehydration in 50 and 70% 2-propanol. The air-dried sections were stored at -20°C until the hybridization. In all these pre-hybridization steps common RNAse-free procedures were adopted to minimize degradation of mRNAs within the tissue sample and to ensure a strong hybridization signal.

Radiolabeled cRNA probes

Levels of c-fos mRNA, oxy mRNA and avp mRNA were examined in the brain sections using in situ hybridization of ^{35}S-labeled RNA probes.

Antisense c-fos riboprobe was transcribed from 1 μg *Pst* I-linearized recombinant clone pBS/rfos with T7 RNA polymerase in the presence of both uridine-5'-[α-^{35}S]thio]triphosphate and cytidine-5'-[α-^{35}S]thio]triphosphate. The resulting cRNA was complementary to positions 583-1250 of clone pc-fos(rat)-1 (Curran *et al.,* 1987). The sense RNA sequence was generated from the same template using T3 RNA polymerase after linearization with *Pvu* II.

Both antisense oxy-riboprobe and antisense avp-riboprobe were generated from *Xho* I-linearized recombinant clone pCRII/OX and pCRII/AVP, respectively, us-

ing Sp6 RNA polymerase. Both sense riboprobes were transcribed from *BamH* I-linearized templates with T7 RNA polymerase.

After transcription, the probes were subjected to mild alkaline hydrolysis as described previously (Angerer *et al*., 1987) and purified on G-50 column (Bio-rad), according to the manufacturer's instructions.

Digoxigenin-labeled cRNA probes

Digoxigenin-labeled probes were synthesized in an in vitro transcription reaction (20 μl) containing 1 μg linearized DNA, 0.1 mM digoxigenin-labeled rUTP (Roche Diagnostic Lab), 10 mM unlabeled rGTP, rATP and rCTP, 20 U RNAse inhibitor and 20 U appropriate RNA polymerase (the same used for radioprobe synthesis). The transcription reaction was run at 37 °C for 3 hours , and DNAse I was added and incubated at 37 °C for an additional 15 min. The DNAse reaction was terminated by adding 2 μl of 0.2 M EDTA and the digoxigenin-labeled probes were then purified on a G-50 column (Bio-rad). After purification, the optical density of the stock labeled probe was determined with spectrophotometer, considering that a reading of 1 at 260 nm wavelength corresponds to approximately 40 μg/ml for single-stranded RNA (Miller *et al*., 1993). Probe was diluted in RNAse-free distilled water to a final concentration of 200 ng/ml in the hybridization cocktail.

Hybridization with radioprobes and autoradiography

The radioprobes were diluted in hybridization buffer (50% deionized formamide, 10% dextran sulfate, 600 mM sodium chloride, 10 mM Tris, pH 7.5, 1 mM Na^{+-} EDTA, 1X Denhardt's solution, 20 mg/ml yeast tRNA, 10% dextran sulfate, and 50% formamide, 100 μg/ml sonicated selmone sperm) to yield concentrations of 75,000 dpm/μ1. Brain sections were coated with 55 μ1 of hybridization solution, slides were coverslipped and incubated for 16 h at 60°C in a humid chamber. Coverslips were removed, and slides were washed in 2X SSC and 1X SSC (20 min each), followed by incubation for 30 min at 37°C in RNase buffer (10 mM Tris, pH 8.0, 0.5 M NaCl, and 1 mM EDTA) containing 1 U/ml RNase T1 and 20 μg/ml RNase A, to reduce background. The slides were washed at room temperature for 5 min in 1X SSC and for 30 min 0.2X SSC , then under high stringency conditions at 60°C in 0.2X SSC (60 min), and at room temperature in 0.2X SSC (30 min). Finally, they were dehydrated in ascending alcohols series and air dried for about 30 min.

Slides were exposed to Kodak Biomax film (Sigma Aldrich) either for 8 hours (in the case of oxy or avp hybridization) or for 3 days (in the case of c-fos hybridization). The films were developed according to the manifacturer's protocol. Coexposure with two calibrated microscales (0.13-35.0 μCi/g and 4.47-400 μCi/g, respectively) of ^{14}C-labeled plastic standards (American Radiolabeled Chemicals

Inc.) permitted quantification of the autoradiographic signal of hybridized brain regions (Miller, 1991). The specificity of the hybridization signal was ascertained by hybridization of adjacent sections labeled with the correnspondingsense probe.

For emulsion autoradiography, selected sets of slides hybridized with c-fos riboprobe were dipped into NTB Kodak autoradiography emulsion (Integra Biosciences, Fernwald, Germany) and exposed for 18 days at 4°C. Autoradiograms were developed according to manifacturer's instructions.

Data analysis

Autoradiography films were scanned (Epson perfection 3200 PHOTO) at high resolution (900 dpi). The Atlas of Paxinos and Watson (1998) was used to define the locations and boundaries of the brain structures of interest (PVN and SON).

Quantitative analysis of hybridized signals on the autoradiographic film was performed using Scion Image software (NIH, USA). Optical densities were converted into radioactivity concentrations by densitometric analysis of ^{14}C-miscoscale standards, so as to create a calibration curve. The film exposure times (i.e. 8 hours or 3 days) were optimized to obtain linear calibration curves with ranges of optical densities that included the optical densities of hybridization signals for each brain area of interest. For each calibration curve we tested the linearity by linear regression and statistical analysis and in all cases we obtained a lin-

ear coefficient $r^2>0.9$ and a non significant ($p>0.05$) departure from linearity. In every brain section, background levels of hybridization were obtained from readings in white matter structures such as the corpus callosum, where minimal binding would be expected to occur and subtracted from the mean reading of the area of interest. Integrated optical density (O.D.) values (radioactivity x area) of hybridized area were measured considering the right and left areas of interest together. Measurements were obtained in at least four consecutive tissue sections containing the desired structure (Lee *et al.,* 2005). Tissue sections were chosen, among those hybridized, to be similar in each experimental group. To chose the proper sections each slide used for the in situ hybridization was examined in phase contrast under a NIKON 80*i* ECLIPSE microscope equipped with a DS-U1 digital camera. Only those brain slices corresponding to the selected set of sections were considered for the quantitative analysis and were selected for emulsion autoradiography. The same microscope was used to visualize autoradiograms under dark-field illumination. For each slice a large image was obtained by stitching separately captured images from the same brain slice acquired at 10X magnification (0.25mm/px at 2560x1920 format quality), by using NIS-elements BR software (NIKON).

Data from quantitative analysis of autoradiography films are reported as the mean percent of the appropriate control subjects' relative integrated density readings ±

SEM. In particular, for purposes of relative comparisons, we established as 100% the average reading from subjects of the FFV-60 min in the time-course experiments, the average reading from subjects of the FFV in the dose-response experiment and average reading obtained from the W-Type V subjects in the experiments on mice. Statistical significance for mRNA expression was determined by two-way or one-way ANOVA, depending from the experimental setting, and multiple comparisons were performed by Tukey's post hoc test. In all instances, statistical significance threshold was set at $p<0.05$.

Hybridization with digoxigenin probes and staining

Hybridization with digoxigenin probes was based on a protocol slightly modified from that described by Miller and colleagues in 1993 (Miller *et al.,* 1993). Digoxigenin probes were diluted in hybridization buffer (50% deionized formamide, 10% dextran sulfate, 600 mM sodium chloride, 10 mM Tris, pH 7.5, 1 mM Na^{+-} EDTA, 1X Denhardt's solution, 20 mg/ml yeast tRNA, 10% dextran sulfate, and 50% formamide, 100 μg/ml sonicated selmone sperm) using 200 ng/ml and further steps were similar to does followed in the radioactive hybridization. For blocking step, the slides were treated with 2% normal goat serium (NGS) and 0,05 % Triton X-100 in 2X SSC 4°C overnight. After the blocking step, slides were washed twice (10 min) in Buffer 1 (0.1 M Tris-HCl, 0.15 M NaCl, pH 7.5) and then incubated for 3 hr at 30°C with the antidigoxigenin antibody, conjugated

to alkaline phosphatase (Roche Diagnostic Lab.), which was diluited (1:500) in buffer 1 containing 1% NGS and 0,3% Triton X-100. Slides were, then, washed in Buffer 1 (10 min), and then washed in Buffer 2 (100 mM Tris-HCl, 100 mM NaCl, 50 mM MgCl2, pH 9.2, 10 min). Digoxigenin-labeled probes were visualized by incubating the slides in a chromogen solution with 340 μg/ml nitroblue tetrazolium chloride, and 175 μg/ml 5-bromo-4-chloro-3-indolyl-phoshate in Buffer 2 overnight at 4 °C. The reaction was blocked by incubating the slides in 10 mM tris-HCl (pH 8) and 1mM EDTA (Buffer 3) at room temperature for at least 2 hours. The slides were dehydrated in ascending alcohols series and air dried for about 30 min. Finally slides were stained with Nissl staining. In particular, sections were incubated with warm 1% cresyl violet acetate (Sigma Aldrich) for 10 min. Stained slides were rinsed in ethanol, cleared in xylene, and coverslipped. Slices were examined in bright-field under a NIKON 80*i* ECLIPSE microscope.

Dual in situ hybridization

Slides were hybridized with a mixture of digoxigenin-oxy-riboprobe and radiolabeled c-fos riboprobe both diluted in the same hybridization buffer (50% deionized formamide, 10% dextran sulfate, 600 mM sodium chloride, 10 mM Tris, pH 7.5, 1 mM Na^{+-}EDTA, 1X Denhardt's solution, 20 mg/ml yeast tRNA, 10% dextran sulfate, and 50% formamide, 100 μg/ml sonicated selmone sperm) at the

same final concentration used in the single hybridization. This probe cocktail was applied to the tissue (60 μl) and sections were coverslipped. Slides were placed in a moist chamber and incubated overnight at 60 °C. After incubation the colocalization of signals were reveled with immunocytochemical detection of digoxigenin –labeled probe as described above and with autoradiographic emulsion for radiolabeled probe into the same slides. Each slide used for the dual in situ hybridization was stained with Nissl staining. For detection of radiolabeled probes with autoradiographic emulsion we capturred an image of each section in dark field while digoxigenin probes were visualized in brightfield microscopy. A merge of the two images of the same section was obtained to evaluate co-localization of the two hybridized probes.

Analysis of feeding behavior

Food intake was recorded with an automated system (PRS Italia), consisting of 6 cages equipped with food trays connected to weight sensors, with lickometers and with sensors for food access. The food trays contained standard chow pellets and were accessible to the rats through a square window in the wall of the cage crossed by an infrared beam (sensor for food access). Each time food was removed from the tray, the computer recorded the episode, as an event of food access and the amount of food retrieved, corrected from the food spillage left in the tray. Food access was detected each time the head of the animal interrupted the

infrared beam of the window, also when no food was taken from the tray. The lickometer counted the licks each time the animal consumed water.

Rats were habituated to the test cages for 2 days prior to trials and had free access to food and water. Experiments with free-feeding rats began at onset of the dark phase and lasted 18 hours. Total food intake was measured and expressed as g Kg^{-1}. Total number of food acces and total number of licks were also measured. Data were analyzed by one way ANOVA and by Tuckey's post hoc test for multiple comparisons.

RESULTS

C-fos hybridization

Representative c-fos mRNA-autoradiography of brain sections obtained from a rat treated with vehicle (panel A) and a rat treated with OEA (10 mg kg-1) (panel B), 60 min before being killed is showed in Figure1. The lack of autoradiographic signal in sections hybridized with c-fos sense probe (representative section in panel C) demonstrates the good quality of c-fos riboprobe.

Analysis of c-fos hybridizated slices showed that the systemic administration of OEA evokes an increase of c-fos mRNA levels in two hypothalamic nuclei: the Paraventricular nucleus (PVN) and the Supraoptic nucleus(SO). For each nucleus the results from densitometric analysis of autoradiography signal were expressed as percentage integrated optical density and analyzed by two-way ANOVA, considering the following factors: treatment and time.

C-fos hybridization in PVN: time course experiment

The results are shown in Figure 1, (panel D). The two-way ANOVA of integrated optical density in the PVN revealed the following results:

F (treatment) = 82,965; df = 1 / 91, p <0.001

F (time) = 10,028; df = 1 / 91, p <0.01

F (treatment x time) = 9,120 df = 1 / 91, p <0.01

The multiple comparisons performed by Tukey's post hoc test showed that the treatment with OEA produces a statistically significant increase in c-fos integrated optical density, 30 minutes (p <0.001) and 1 hour after OEA administration (p <0.001).

C-fos hybridization in SO: time course experiment

The results are shown in Figure 1, (panel E). The two-way ANOVA of integrated optical density in SO provided the following results:

F (treatment) = 14,382; df = 1 / 47, p <0.001

F (time) = 1,195, df = 1 / 47; n.s.

F (treatment x time) = 4,838 df = 1 / 47, p <0.05

The multiple comparisons performed by the Tukey's test showed that the OEA treatment produces a statistically significant increase in c-fos integrated optical density 1h (but not 30 minutes) after the administration (p <0.001).

Oxytocin hybridization

Representative oxy mRNA-autoradiography of brain sections obtained from a rat treated with vehicle (panel A) and a rat treated with OEA (10 mg kg-1) (panel B), 60 min before being killed is showed in Figure 2. The hybridization with the antisense oxy mRNA probe has shown a highly specific strong hybridization in the PVN and SO nuclei. The lack of autoradiographic signal in sections hybridized with oxy sense probe (representative section in panel **C**) demonstrates the good quality of oxy riboprobe.

For each nucleus the results from densitometric analysis of autoradiography signal were expressed as percentage integrated optical density and analyzed by two-way ANOVA, considering the following factors: treatment and time.

OXY Hybridization in the PVN: time course experiment

The results are shown in Figure 2, (panel D). The two-way ANOVA of integrated optical density in the PVN provided the following results:

F (treatment) = 4,650, df = 1 / 230, $p < 0.05$

F (time) = 4,289, df = 2 / 230, $p < 0.05$.

F (treatment x time) = 2,353 df = 2 / 230; n.s.

The multiple comparisons performed by the Tukey's test showed that OEA treatment produces a statistically significant increase of integrated optical density ($p < 0.05$) 1h after OEA administration. No alteration has been observed 2 hours and 4 hours after OEA administration.

OXY Hybridization in the SO: time course experiment

The results are shown in Figure 2, (panel E). The two-way ANOVA of integrated optical density in the SO revealed the following results:

F (treatment) = 14,505; df = 1 / 198, $p < 0.001$

F (time) = 0,094, df = 2 / 198; n.s.

F (treatment x time) = 1,098 df = 2 / 198; n.s.

The multiple comparisons performed by Tukey's test showed that OEA administration produces a statistically significant increase of integrated optical density 1 hour ($p < 0.05$) and 2 hours ($p < 0.05$) after treatment, while no alteration has been observed after 4 hours.

AVP hybridization

Representative avp mRNA-autoradiography of brain sections obtained from a rat treated with vehicle (panel A) and a rat treated with OEA (10 mg kg-1) (panel B),

60 min before being killed is showed in Figure 3. The hybridization with the antisense avp mRNA probe has shown a highly specific strong hybridization in the PVN and SO nuclei. The lack of autoradiographic signal in sections hybridized with avp sense probe (representative section in panel C) demonstrates the good quality of avp riboprobe.

For each nucleus the results from densitometric analysis of autoradiography signal were expressed as percentage integrated optical density and analyzed by two-way ANOVA, considering the following factors: treatment and time.

AVP hybridization in the PVN: time course experiment

The results are shown in Figure 3, (panel D). The two-way ANOVA of integrated optical density in the PVN revealed the following results:

F (treatment) = 0,004, df = 1 / 148; n.s.

F (time) = 5,563, df = 2 / 148, $p < 0.01$

F (treatment x time) = 1,349 df = 2 / 148; n.s.

These results indicate that OEA treatment does not affect the avp mRNA expression in the PVN nucleus.

AVP hybridization in the SO: time course experiment

The results are shown in Figure 3, (panel E). The two-way ANOVA of integrated optical density in the SO provided the following results:

F (treatment) = 0,821, df = 1 / 184; n.s.

F (time) = 5,968, df = 2 / 184, p <0.01

F (treatment x time) = 0,208 df = 2 / 184; n.s.

These results indicate that OEA treatment does not affect the mRNA expression of avp in the SO nucleus.

OXY Hybridization in the PVN: dose-response experiment

The results are shown in Figure 4, (panel A). The one-way ANOVA of integrated optical density in the PVN revealed the following results: F = 11,83, df = 3 / 127, p <0.01.

The multiple comparisons performed by Tukey's test showed that the treatment with OEA 10 mg/kg, produces a statistically significant increase of integrated optical density (p <0.01). No significant increase of the integrated optical density was found following the administration of OEA at either 5 mg/kg or 20 mg/kg .

OXY Hybridization in the SO: dose-response experiment

The results are shown Figure 4, (panel B). The one-way ANOVA of integrated optical density in SO revealed the following results: $F = 6{,}417$, $df = 3 / 153$, $p < 0.001$ The multiple comparisons performed by the Tukey's test showed that OEA treatment produces a statistically significant increase of integrated optical density when administered at the dose of 10 mg/kg ($p<0.01$). No significant increase of the integrated optical density was found after 5 mg/kg and 20 mg/kg OEA injection.

Dual in situ hybridization

The analysis of brain slices hybridized with both c-fos and oxy probes has shown that >90% of c-fos hybridization coincides with the oxy hybridization in animals treated with OEA (10 mg kg^{-1}), 60 min before being killed (Figure 5).

Oxytocin hybridization in PPAR-$\alpha^{-/-}$ and wild type mice

Representative oxy mRNA-autoradiography of brain sections obtained from: free-feeding wild type mice treated either with vehicle (panel A) or OEA (10 mg kg-1) (panel B) and free-feeding PPAR-alpha $^{-/-}$ mice treated either with vehicle (panel E) or OEA (10 mg kg-1) (panel F), 60 min before being killed is showed in Fig-

ure 6. The hybridization with the antisense oxy mRNA probe has shown a highly specific strong hybridization in the PV and SO nuclei.

For each nucleus the results from densitometric analysis of autoradiography signal were expressed as percentage integrated optical density and analyzed by two-way ANOVA, considering the following factors: strain and treatment.

OXY Hybridization in the PVN of PPAR-$\alpha^{-/-}$ and wild type mice

The results are shown in Figure 6, (panel C and panel G). The two-way ANOVA of integrated optical density in the PVN of PPAR-$\alpha^{-/-}$ and wild type mice revealed the following results:

F (strain) = 0.263, df = 1 / 69, n.s.

F (treatment) = 4.638, df = 1 / 69, $p < 0.05$

F (strain x treatment) = 2,313 df = 1 / 69, n.s.

The multiple comparisons performed by Tukey's test showed that OEA administration produces a statistically significant increase of integrated optical density in the PVN of wild type mice ($p < 0.05$, panel **C**), while no alteration has been observed in PPAR-$\alpha^{-/-}$ mice (panel **G**).

OXY Hybridization in the SO of PPAR-$\alpha^{-/-}$ and wild type mice

The results are shown in Figure 6, (panel D and panel H). The two-way ANOVA of integrated optical density in the SO of PPAR-$\alpha^{-/-}$ and wild type mice revealed the following results:

F (strain) = 0.001, df = 1 / 66, n.s.

F (treatment) = 2.845, df = 1 / 66, n.s

F (strain x treatment) = 0.535 df = 1 / 66, $p < 0.05$

The multiple comparisons performed by Tukey's test showed that OEA administration produces a statistically significant increase of integrated optical density in the SO of wild type mice ($p < 0.05$, panel D), while no alteration has been observed in PPAR-$\alpha^{-/-}$ mice (panel H).

Feeding behavior analysis

The results are shown in Figure 7. The statistical analysis of 18-hour cumulative food intake provided the following results: F = 6,093, df = 3 / 31, $p < 0.01$. The multiple comparison test showed that OEA significantly inhibited food consumption in rats ($p < 0.01$), while the administration of atosiban 30 minutes before

OEA, completely reverted its effects, without producing per se any alteration of cumulative food intake.

OEA treatment did not affect drinking or food access (data not shown).

DISCUSSION

A large body of evidence indicate that the anorexiant effects of OEA are mediated by the activation of peripheral PPAR-alpha receptors, but the central mechanisms downstream to this activation are still unclear. Brain regions that area activated in rats after OEA treatment have been mapped on the basis of neuronal expression of c-*fos* mRNA, a mRNA product of the early response gene c-*fos*. OEA treatment increased mRNA c-fos expression in two important hypothalamic nuclei involved in the energy balance: the paraventricular nucleus (PVN) and the sopraoptic nucleus (SO) (Rodriguez de Fonseca *et al*., 2001). In agreement with these previous observations we found an increase of c-fos mRNA in both nuclei that is evident 30 min after OEA systemic administration, but reaches its maximum at 60 min, decreasing at 120 and 240 minutes (data not shown). The magnocellular components of both nuclei release oxy and avp, two of the anorectic hypothalamic neuropeptides and project their axons to the posterior pituitary where they secrete oxy and avp into the periphery. Dendritic oxy acts locally to facilitate oxy neuron activity but also diffuse to distant sites as the amygdala. Smaller oxy neurons of the PVN project centrally to various hypothalamic, limbic and brainstem regions. So central oxy system can provide a multi-level controlling influence on other brain regions and has an important role in the regulatory neuronal network

mediating satiety. Our hypothesis was that the increased c-fos mRNA in the PVN and SON might be paralleled by increase of oxy mRNA levels in the same neurons. To test such hypothesis we performed a time-course and a dose response study in rats, systemically administered with OEA. We found that OEA treatment does cause an increase of oxy mRNA in the PVN and SO nuclei, and such increase is highest at 60 minutes after treatment and is maximal at the dose of 10 mg kg^{-1}. The lack of effects at the highest dose of OEA (20 mg kg^{-1}) is accompanied by the lack of behavioral selectivity of the drug at this dose. In fact, while no effects of OEA on motor behavior and drinking activity are observed at both 5 and 10 mg doses, a slight motor inhibition and a decrease of water consumption can be observed in rats treated with the highest dose of the compound (Rodriguez de Fonseca *et al*., 2001). We therefore, hypothesize that at this dosage other neuronal signals might be modulated that could differently affect oxy mRNA levels in the PVN and SO. OEA effects on oxy mRNA appears highly selective, as we did not detect any alteration of avp mRNA in the same brain regions where the increase of oxy mRNA was observed. Moreover, by dual in situ hybridization we verified that OEA causes an increase of oxy mRNA expression in the same neurons expressing higher levels of c-fos mRNA, thus suggesting that the activation of these neurons is accompanied to increased oxytocinergic tone.

Although OEA may bind to multiple receptors (Ahern *et al.,* 2003; Overton *et al.,* 2006), different lines of evidence indicate that PPAR-α mediates the effects of this compound on energy homeostasis (Fu *et al.,* 2003). PPAR-α knockout mice do not respond to OEA or synthetic PPAR-α agonists (Fu *et al.,* 2003). Long-term OEA administration causes metabolic changes similar to those produced by PPAR-α agonists, consisting of decreased serum cholesterol and triglyceride levels in genetically obese rats (Fu *et al.,* 2005). PPAR-α receptors are expressed also in the central nervous system, however some indications suggest that the anorexiant effect of OEA is mainly peripheral. In fact, OEA does not affect food intake when injected into the rat brain ventricles, and its anorexic actions are prevented when peripheral sensory fibers are removed (Rodriguez de Fonseca, *et al.,* 2001). Interestingly, we found that a significantly increase of oxy mRNA in the PVN and SO nuclei can be observed in wild-type mice treated with OEA, whereas any alteration of oxy mRNA levels can be detected in PPAR-alpha$^{-/-}$ mice, following OEA administration. These observation highlight the correlation between oxy mRNA increase in the hypothalamus and the anorexiant effects of OEA, since they are both absent in PPAR-alpha$^{-/-}$ mice.

To further test the occurrence of any relationship between oxytocinergic signalling and the inhibition of food intake induced by OEA administration, we tested whether the oxy antagonist atosiban could block OEA effects on feeding. The re-

sults of the behavioral experiment in rats confirmed our hypothesis, showing how a systemic dose of atosiban that per se does not produce any effect on feeding, can completely reverse the effects of OEA when it is pre-administered to rats receiving OEA.

Similar findings on food intake and oxy involvement in the hypothalamus were observed also in the case of the anorexiant action of the CB1 antagonist rimonabant (SR141716A) (Verty *et al*., 2004). The study by Verty suggested an interplay between the endocannabinoid system and the oxytocinergic system in the hypothalamus. In fact, rimonabant and oxy administration in the hypothalamus were found to synergictically interact in reducing eating and CB1 receptor signaling resulted necessary to prevent oxy from altering food intake.

As mentioned before, OEA does not activate CB1 receptors, nor it can be considered an endocannabinoid, since its actions in vivo are drastically different from those produced by cannabinoid agonists. However, OEA can be synthetized and released, as well as hydrolyzed, together with anandamide, since they share several metabolic pathways. Anandamide has opposite effects on feeding behavior, as, similarly to THC and other cannabinomimetic compounds, it can stimulate food intake.

Rimonabant shares with OEA several effects on energy balance and food intake. However, although rimonabant acts on eating behavior predominantly blocking

central CB1 receptors, the actions of OEA on feeding are mostly peripheral. This difference is of crucial importance since the central effects of CB1 blockade are also responsible for the psychiatric side effects of rimonabant that caused its withdrawal from the market.

OEA effects on oxy release in the PVN and SO are likely due to indirect activation on the hypothalamic nuclei, as suggested by previous findings showing an increase of c-fos mRNA in the NTS after OEA administration (Rodriguez de Fonseca *et al.,* 2001). Thus, OEA might represent a novel pharmacological tool that simulates the effects of rimonabant on energy homeostasis, without blocking CB1 receptors directly but probably counterbalancing the effects of endogenous anandamide. Oxy release in the PVN and SO might represent one of the possible common target where such balance occurs and that is involved in the effects on feeding.

REFERENCES

Ahern G.P. (2003) "Activation of TRPV1 by the satiety factor oleoylethanolamide". J. Biol. Chem., 278, 30429-30434.

Amico, J.A., Vollmer, R.R., Cai, H.M., Miedlar, J.A., Rinaman, L., (2005). "Enhanced initial and sustained intake of sucrose solution in mice with an oxytocin gene deletion". Am J Physiol 289, R1798–1806.

Angerer, L. M., Cox, K. H., and Angerer, R. C. (1987). "Demonstration of tissue-specific gene expression by in situ hybridization." Methods Enzymol, 152, 649-61.

Blevins, J.E., Schwartz, M.W., Baskin, D.G., (2004). "Evidence that paraventricular nucleus oxytocin neurons link hypothalamic leptin action to caudal brain stem nuclei controlling meal size". Am J Physiol Regul Integr Comp Physiol 287, R87-96.

Curran, T., Gordon, M. B., Rubino, K. L., and Sambucetti, L. C. (1987). "Isolation and characterization of the c-fos(rat) cDNA and analysis of post-translational modification in vitro." Oncogene, 2(1), 79-84.

Desvergne, B., and Wahli, W. (1999). "Peroxisome proliferator-activated receptors: nuclear control of metabolism." Endocr Rev, 20(5), 649-88.

Fu J., Gaetani S., Oveisi F., Lo Verme J., Serrano A., Rodríguez De Fonseca F.Rosengarth A., Luecke H., Di Giacomo B., Tarzia G., Piomelli D. (2003). "Oleylethanolamide regulates feeding and body weight through activation of the nuclear receptor PPAR-alpha". Nature, 425, 90- 93.

Fu J., Oveisi F., Gaetani S., Lin E., Piomelli D. (2005). "Oleoylethanolamide, an endogenous PPAR-alpha agonist, lowers body weight and hyperlipidemia in obese rats". Neuropharmacology, 48, 1147-1153.

Giuffrida, A., Rodrıguez de Fonseca, F., Pomelli, D. (2000). "Quantification of bioactive acylethanolamides in rat plasma by electrospray mass spectrometry". Anal Biochem 280, 87–93.

Hillebrand, J. J., de Wied, D., and Adan, R. A. (2002). "Neuropeptides, food intake and body weight regulation: a hypothalamic focus." Peptides, 23(12), 2283-306.

Lee, P. R., Brady, D. L., Shapiro, R. A., Dorsa, D. M., and Koenig, J. I. (2005). "Social interaction deficits caused by chronic phencyclidine administration are reversed by oxytocin." Neuropsychopharmacology, 30(10), 1883-94.

Ludwig, M., and Leng, G. (2006). "Dendritic peptide release and peptide-dependent behaviours." Nat Rev Neurosci, 7(2), 126-36.

Mantella, R.C., Vollmer, R.R., Rinaman, L., Li, X,, Amico, J.A. (2004). "Enhanced corticosterone concentrations and attenuated Fos expression in the medial amygdala of female oxytocin knockout mice exposed to psychogenic stress". Am J Physiol. 287**,** R1494–1504.

Miller, J.A. (1991). "The calibration of 35S or 32P with 14C-labeled brain paste or 14C-plastic standards for quantitative autoradiography using LKB Ultrofilm or Amersham Hyperfilm". Neurosci Lett. 121, 211-214.

Miller, M.A., Kolb, P.E., Raskind, M.A. (1993). "A method for simultaneous detection of multiple mRNAs using digoxigenin and radioisotopic cRNA probes". J. Histochem. Cytochem. 41, 1741-1750.

Moore, M.R., Black, P.M. (1991). "Neuropeptides". Neurosurg. 14, 97-110.

Overton H.A., Babbs A.J., Doel S.M., Fyfe M.C., Gardner L.S., Griffin G., Jackson H.C., Procter M.J., Rasamison C.M., Tang-Christensen M., Widdowson P.S., Williams G.M., Reynet C. (2006). "Deorphanization of a G protein-coupled receptor for oleoylethanolamide and its use in the discovery of small-molecule hypophagic agents". Cell Metab., 3, 167-175.

Rinaman, L., Vollmer, R.R., Karam, J., Phillips, D., Li, X., Amico, J.A. (2005). "Dehydration anorexia is attenuated in oxytocin-deficient mice". J Physiol Regul Integr Comp Physiol. 288, R1791-1799.

Rodríguez de Fonseca F., Navarro M., Gómez R., Escuredo L., Nava F., Fu J., Murillo-Rodríguez E., Giuffrida A., LoVerme J., Gaetani S., Kathuria S., Gall C., Piomelli D. (2001). 2001. "An anorexic lipid mediator regulated by feeding". Nature, 414, 209-12,

Sabatier, N. (2006). "Alpha-Melanocyte-stimulating hormone and oxytocin: a peptide signalling cascade in the hypothalamus". J Neuroendocrinol. 18, 703-710.

Verty AN, McFarlane JR, McGregor IS, Mallet PE. (2004). "Evidence for an interaction between CB1 cannabinoid and oxytocin receptors in food and water intake". Neuropharmacology. Sep;47(4):593-603

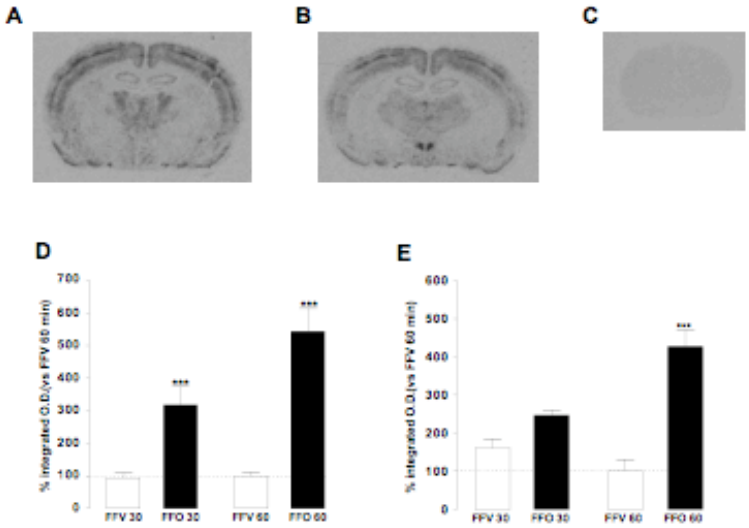

Figure 1. Representative c-fos mRNA-autoradiography of brain sections obtained from a rat treated with vehicle (panel **A**) and a rat treated with OEA (10 mg kg-1) (panel **B**), 60 min before being killed. The lack of autoradiographic signal in sections hibridized with c-fos sense probe (representative section in panel **C**) demonstrates the specificity of hybridization for c-fos mRNA showed in panels A and B.

Quantitative analysis of c-fos mRNA in the PVN (panel **D**) and SO (panel **E**) of FFV and FFO rats treated either 30 min or 60 min before being killed. *** $p<0.001$ vs respective control (Tukey's test)

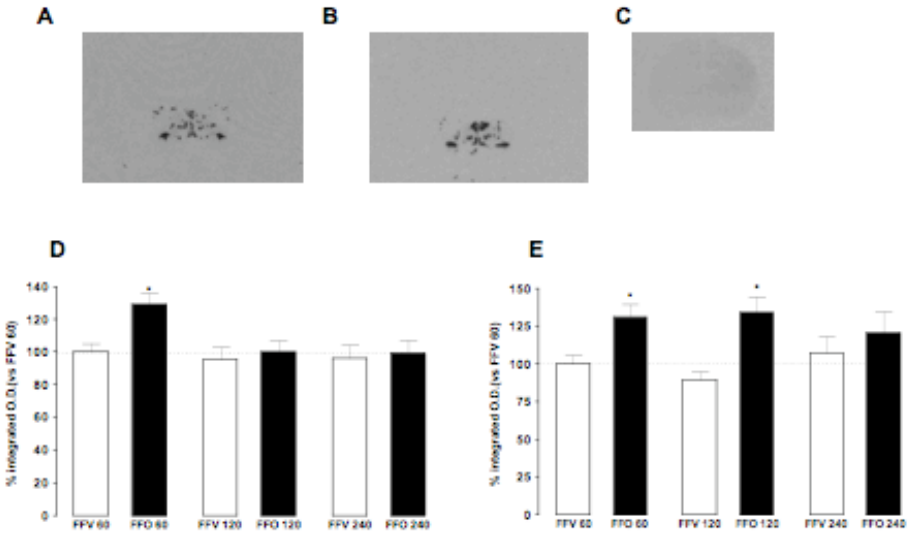

Figure 2. Representative oxy mRNA-autoradiography of brain sections obtained from a rat treated with vehicle (panel **A**) and a rat treated with OEA (10 mg kg-1) (panel **B**), 60 min before being killed. The lack of autoradiographic signal in sections hibridized with oxy sense probe (representative section in panel **C**) demonstrates the specificity of hybridization for oxy mRNA showed in panels A and B. Quantitative analysis of oxy mRNA in the PVN (panel **D**) and SO (panel **E**) of FFV and FFO rats treated either 60 min, 120 min, or 240 min before being killed.
* $p<0.05$ vs respective control (Tukey's test)

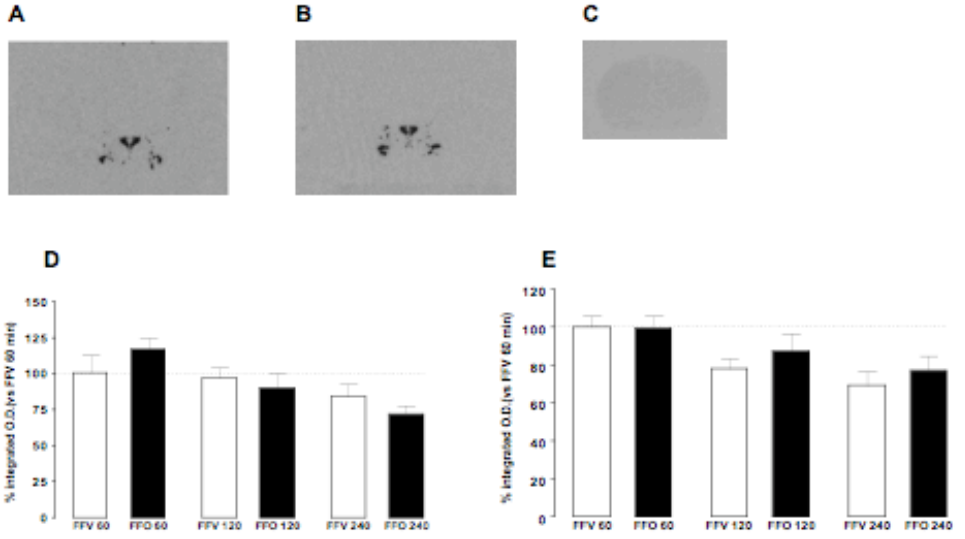

Figure 3. Representative avp mRNA-autoradiography of brain sections obtained from a rat treated with vehicle (panel **A**) and a rat treated with OEA (10 mg kg-1) (panel **B**), 60 min before being killed. The lack of autoradiographic signal in sections hibridized with avp sense probe (representative section in panel **C**) demonstrates the specificity of hybridization for avp mRNA showed in panels A and B.

Quantitative analysis of avp mRNA in the PVN (panel **D**) and SO (panel **E**) of FFV and FFO rats treated either 60 min, 120 min, or 240 min before being killed.

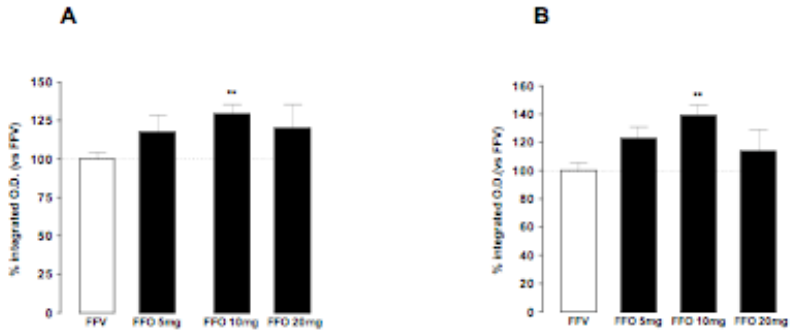

Figure 4. Quantitative analysis of oxy mRNA in the PVN (panel **A**) and SO (panel **B**) of FFV and FFO rats treated 60 min before being killed. OEA was administered at 5, or 10 or 20 mg kg^{-1}.
** $p<0.01$ vs respective control (Tukey's test)

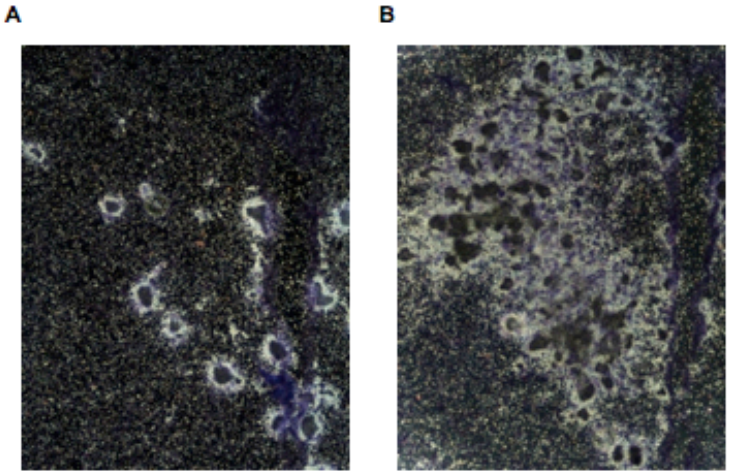

Figure 5. Representative merged image of hybridized digoxigenin-labeled probe for oxy mRNA and hybridized ^{35}S-radiolabeled probe for c-fos mRNA. (**A**) section from FFV 60 min; and (**B**) section from FFO 60 min.

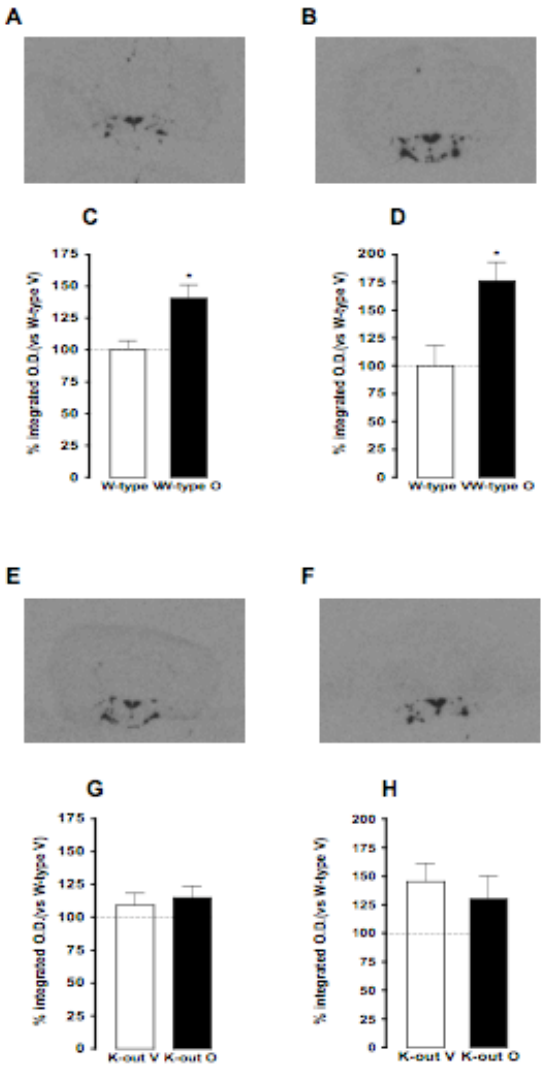

Figure 6. Representative oxy mRNA-autoradiography of brain sections obtained from: free-feeding wild type mice treated either with vehicle (panel **A**) or OEA (10 mg kg-1) (panel **B**) and free-feeding PPAR-alpha $^{-/-}$ mice treated either with vehicle (panel **E**) or OEA (10 mg kg-1) (panel **F**), 60 min before being killed.
Quantitative analysis of oxy mRNA in the PVN (panel **C**) and SO (panel **D**) of W-type V and W-type O mice, and quantitative analysis of oxy mRNA in the PVN (panel **G**) and SO (panel **H**) of K-out V and K-out O mice , 60 min before being killed.
* $p<0.05$ vs respective control (Tukey's test)

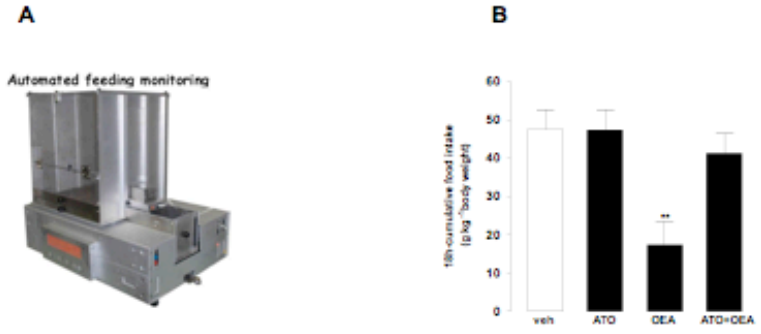

Figure 7. Free-feeding rats were habituated to test cages (panel **A**) for two days. On test day rats were divided into four hroups:
veh: rats treated with saline and with vehicle
ATO: rats treated with atosiban (ATO, 1 mg kg^{-1} i.p.) and vehicle
OEA: rats treated with saline and with OEA (10 mg kg^{-1} i.p.)
ATO+OEA: rats treated with ATO (1 mg kg^{-1} i.p.) and with OEA (10 mg kg^{-1} i.p.)
18-hour-cumulative food intake is reported in panel **B**.
** p<00.1 vs veh (Tukey's test)

CHAPTER IV

OEA AND BEHAVIOURAL SEQUENCY OF SATIETY

INTRODUCTION:

A plethora of drugs exist that inhibit food intake when administered to experimental animals. One of the most contentious issues in the psychopharmacology of appetite concerns the identification of mechanism underlying an observed reduction of eating. It cannot be denied that many chemicals could suppress eating by producing adverse physiological effects such as pain, or illness, or by altering neurochemical systems or behavioral dispositions so as to prevent the normal expression of appetite. Because animals cannot report their aversive side effects to the experimenter, the maintenance of a normal structure in strings of behavioral acts may be used as a means of verifying normal physiology. For over 20 years researchers have argued that the structure of behavior can be used as a marker of the nonphysiological effects of drugs on food intake. The utility of the behavioural sequence of satiety (BSS) rests initially on the validity of behavior as an indicator of toxic, pathologic, or nonphysiological events. Monitoring animal beha-

vior, inducing feeding, and nonfeeding activities could provide a powerful biobehavioral assay of drug action on appetite. Using this biobehavioral assay of feeding avoids problems of model validity, as it does not rely on modeling the human condition, but uses the animal's natural behavioral register as the yardstick of relevance (Halford *et al*., 1998).

The commonest dependent variable recorded in animal studies aimed at understanding drug effects on feeding is amount of food eaten by the subjects. Food intake is the result of the interplay between internal and external variables (Berthoud *et al.,* 2002) and therefore, per se, not helpful to explain the mechanism affecting food consumption. It has been suggested that important information on the action of compounds inducing changes in appetite can be obtained through a more detailed analysis of feeding behavior. In rodents, the BSS represents the natural progression from eating to resting, through active grooming, in its formal and operational definition (Antin *et al.,* 1975).

Cannabinoid CB1 inverse agonist such as rimonabant SR141716A (Rinaldi *et al*., 1994) hold therapeutic promise as appetite suppressants, but the extent to which non-motivational factors contribute to their anorectic effects is not fully known. Examination of the BSS in rats, the orderly progression from eating to postprandial grooming and then resting, has revealed that this compounds preserves the order of events but differ markedly from natural satiation . The most notable

difference is that grooming (particularly scratching) is profoundly enhanced at anoretic doses, while eating and resting are diminished, raising the possibility that anorectic effect is simply secondary to the grooming effect (Hodge *et al*., 2008).

Acomplia is a medicine containing the active substance rimonabant. Acomplia was authorised in the European Union since June 2006 and was marketed in 18 EU Member States. Rimonabant was also authorised as Zimulti, but this product was not marketed in the EU. Acomplia can cause psychiatric side effects, especially depression, since its initial assessment. Because patients at an elevated risk of developing psychiatric disorders could not be identified, the Committee concluded that introducing further restrictions to the use of the medicine would be unlikely to reduce the risk to an acceptable level. Therefore, the Committee concluded that the benefits of Acomplia no longer outweigh its risks, and recommended that the marketing authorisation for the medicine should be suspended across the EU (EMEA London 23 October).

In this scenario, several researcher are actually focusing on the development of novel CB1 antagonists that could not cross the blood brain barrier, thus avoiding the central effects displayed by rimonabant and possibly responsible of the adverse side effects. Although several metabolic positive effects of accomplia are raleted to CB1 antagonism at the periphery, the main effects on food intake appears to be centrally mediated. Thus, the question arises to whether a novel CB1 anta-

gonist that cannot block central CB1 receptors might still modulate eating behavior in laboratory animals as well as in humans. In this respect OEA might represent a better candidate for the development of novel therapeutic tools for obesity and over-eating. In fact, the effects of OEA appear to be mostly peripheral, while clearly influencing feeding behavior.

In this study we compared the behavioral effects of OEA to those of rimonabant in mice subjected to the analysis of BSS.

METHODS

Animals and experimental conditions

Animals were housed under controlled 12-h light–dark cycle (7:00 A.M.–7:00 P.M.), and allowed free access to food and water in their home cage. The basic diet consisted of standard laboratory dry food pellets (Mucedola s.r.l.). All experiments took place during the dark cicle in a soundproof enviroment. Thirty-eight male (C57/Bl6) mice were used for the study. The animals, weighing 28±0.5 g on arrival, were purchased at approximately 10 weeks of age from Charles River (Como, Italy). All animals used were maintained in accordance with the regulations of the European Communities Council Directive (86/EEC) and approved by the Italian Government (Coccurello *et al*., 2008).

Treatments

Oleyolethanolamide (OEA) was synthesized in the laboratory (Giuffrida *et al*., 2000), dissolved in saline/polyethylene glycol/Tween 80 (90/5/5, v/v; 2 ml Kg^{-1}) and administered, 10 min before dark onset, by intraperitoneal (i.p.) injection at dose of 5 and 10 mg Kg^{-1} to free-feeding mice. Rimonabant (SR141716A), dissolved in the same vehicle of OEA, was administered (i.p.) at the same doses (5 and 10 mg Kg^{-1}) to free-feeding mice. Control animals received an i.p. injection of vehicle.

Experimental procedure

Before starting the pharmacological study, mice were habituated to a semi-liquid diet (wet mash). The diet was made up of a mix of one part ground standard dry powdered food pellets and water (Coccurello *et al*., 2008). Furthermore, the consistency of mash virtually eliminates spillage and prevents animals from removing food to hoard or eat elsewhere (Halford *et al*., 1998). The food pot, weighed immediately prior testing, was positionated in the opposite side of the bottle of water in the cage. To familiarize the animals to the new diet, fresh meals were prepared and offered for one week before administration of OEA and SR141716A. The experimental phase started at the end of final habituation trials and was conducted according to a within-subjects (crossover) design. The treatment condition was determined by Latin Square. One hour before each recording session, mice were food deprived while water remained available. To analyze feeding behavior, subjects were individually placed in a new test cage strewn with the home cage bedding and freely allowed to access the diet up to 45 min. Each food container was preweighed, and the difference between initial and final food container weights was the measure of wet mash intake.

Behavioral satiety sequence analysis

Data were collected between 19:00 and 20:00 p.m. in a soundproof cubicle equipped with a video-recording camera. Test DVDs recorded were scored blind by a highly trained observer using software OBSERVER.

After presentation of wet mash, the behavioural sequence was recorded by observing each mouse for 45 min and allocating its current behaviour to one of five categories. The behavioural categories were: 'duration of eating': holding or ingesting of food; 'active': moving, rearing and other behaviour patterns not defined elsewhere; 'groom': body care movements using mouth or forelimbs; and 'inactive': characterized as an absence of movement with a resting posture, with or without eye closure (Somerville *et al*., 2007). 'Eating latency': time to begin eating measured from initial contact with food.

Data analysis

One way ANOVA was used to analyze duration of eating of observed behavior with drugs (2 different doses) during the 45 min test session, multiple comparison were performed by Tukey's post hoc test. In all instances, statistical significance threshold was set at $p<0.0001$.

RESULTS AND DISCUSSION

Analysis of the behavioral patterns over the course of the 45 min session showed a significant decrease in eating time of the 5 mg/kg and 10 mg/kg OEA group in comparison to vehicle mice (Figure 1 panel A, B and C). Eating time decrease was similar to 5 mg/kg and 10 mg/kg SR141716A group in comparison to vehicle mice (Figure 2 panel A, B and C).

Food intake was significantly affected by drug treatment: the one-way ANOVA revealed the following results: $F=9.723$; $df= 4 / 36$; $p<0.0001$

The multiple comparisons performed by Tukey's post hoc test showed that the treatment with OEA 5 mg/kg and OEA 10 mg/kg produced a statistically significant decrease in eating time (respectively $p <0.01$ and $p< 0.001$ vs vehicle). Also SR171416A 5 mg/kg and 10 mg/kg confirmed a statistically significant decrease in eating time respectively $p<0.001$ and $p<0.001$ vs vehicle; no differences in the amount of the food eaten were found between 5 mg/kg and 10 mg/kg of OEA or SR141716A administered mice (Figure 3).

The BSS has been extensively used to characterize the influence of pharmacological and non pharmacological manipulation on the normal pattern of behaviours associated with feeding (Halford *et al.,* 1998). Throughout its study it is possible to accurately monitor the development and the behavioural structure of the satiation process. Indeed, in basal conditions, the ingestion of food gradually induces

satiation, a process demonstrated by the replacement of feeding with other non-feeding activities (such as grooming), ending in a long-lasting resting period (Coccurello *et al.,* 2008). To our knowledge, this is the first study analyzing the structure of BSS after OEA administration.

OEA caused a marked increased of the latency to the first food approach. This effect was similar to those produced by rimonabant and is in accordance with previous studies (Gaetani *et al.,* 2003). Interestingly, while OEA did not affect grooming behaviour, rimonabant caused an increase of it, as previously reported. On the other hand, the decrease of food intake elicited by OEA and rimonabant was similar, thus suggesting that OEA might simulate the positive effects of Rimonabant on feeding, avoiding its ambiguous effects on other aspects of animal behaviour that might be predictive of adverse side effects in humans.

We, theefore suggest that OEA might represent a valid alternative approach to peripherally acting novel CB1 antagonists.

REFERENCES

Antin J., Gibbs J., Holt J., Young R. C., Smith G. P. (1975). "Cholecystokinin elicits the complete behavioral sequence of satiety in rats". J Comp. Physiol. Psychol., 89: 784-790

Berthoud, H.R. (2002). "Multiple neural systems controlling food intake and body weight". Neurosci. Biobehav. Rev., 26: 393-428

Coccurello R, D'Amato FR, Moles A. (2008). "Chronic administration of olanzapine affects Behavioral Satiety Sequence and feeding behavior in female mice". Eat Weight Disord. Sep;13(3):e55-60.

Gaetani S, Oveisi F, Piomelli D. (2003). "Modulation of meal pattern in the rat by the anorexic lipid mediator oleoylethanolamide". Neuropsychopharmacology. Jul;28(7):1311-6

Giuffrida, A., Rodrıguez de Fonseca, F., Piomelli, D. (2000). "Quantification of bioactive acylethanolamides in rat plasma by electrospray mass spectrometry". Anal Biochem 280, 87–93.

Halford JC, Wanninayake SC, Blundell JE.(1998). "Behavioral Satiety Sequence (BSS) for the Diagnosis of Drug Action on Food Intake". Pharm Biochem and Behavior 61, 159–168.

Hodge, J., Bow, J.P., Plyler, K.S., Vemuri, V.K., Wisniecki, A., Salomone, J.D., Makriyannis, A., McLaughlin, P.J. (2008). "The endocannabinoid CB1 receptor inverse agonist AM 251 and antagonist AM 4113 produce similar effects on the behavioral satiety sequence in rats". Behavioral Brain Research 193, 298-305.

Rinaldi-Carmona, M., Barth, F., Héaulme, M., Shire, D., Calandra, B., Congy, C., Martinez, S., Maruani, J., Nélia, G., Caput, D. (1994). "SR141716A, a potent and selective antagonist of the brain cannabinoid receptor" . FEBS Lett. 350, 240-244.

Somerville, E.M., Horwood, J.M., Lee, M.D., Kennett, G.A. Clifton, P.G. (2007). "5-HT(2C) receptor activation inhibits appetitive and consummatory comp nents of feeding and increases brain c-fos immunoreactivity in mice". Eur J. Neurosci. 25, 3115-3124.

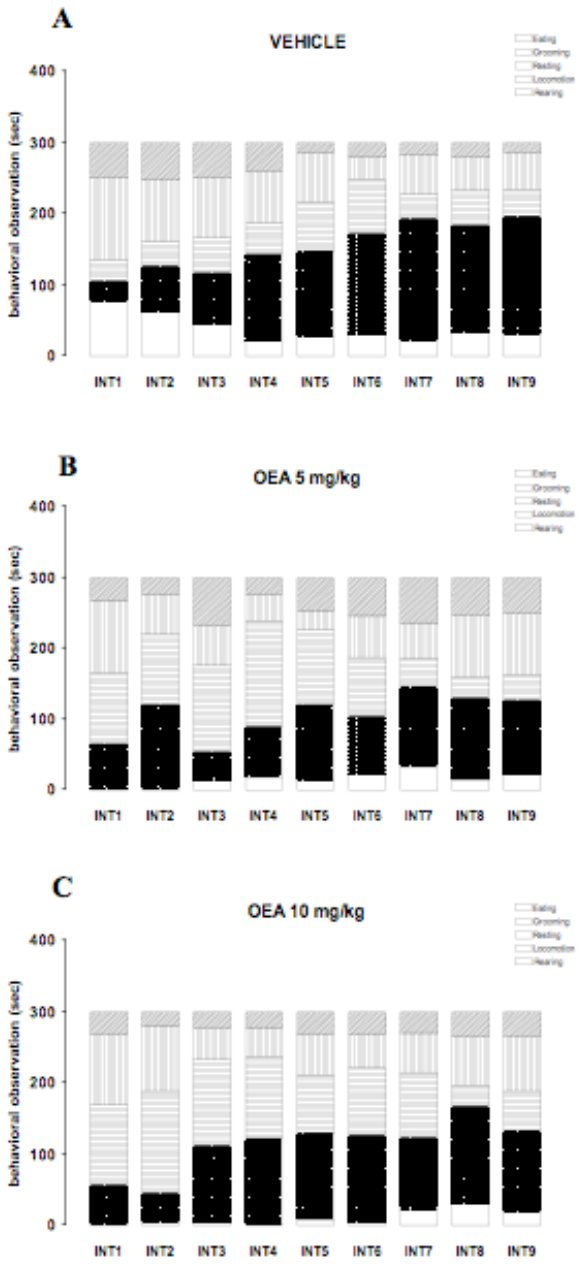

Figure 1. Temporal trend of eating, grooming, resting, locomotion and rearing duration. Panels show the results for vehicle group (A), OEA (5 mg/kg) (B) and OEA (10 mg/kg) (C) administered mice. Represented on the X-axes are 9 time bins of 5 min each for a total 45 min of behavioral observation.

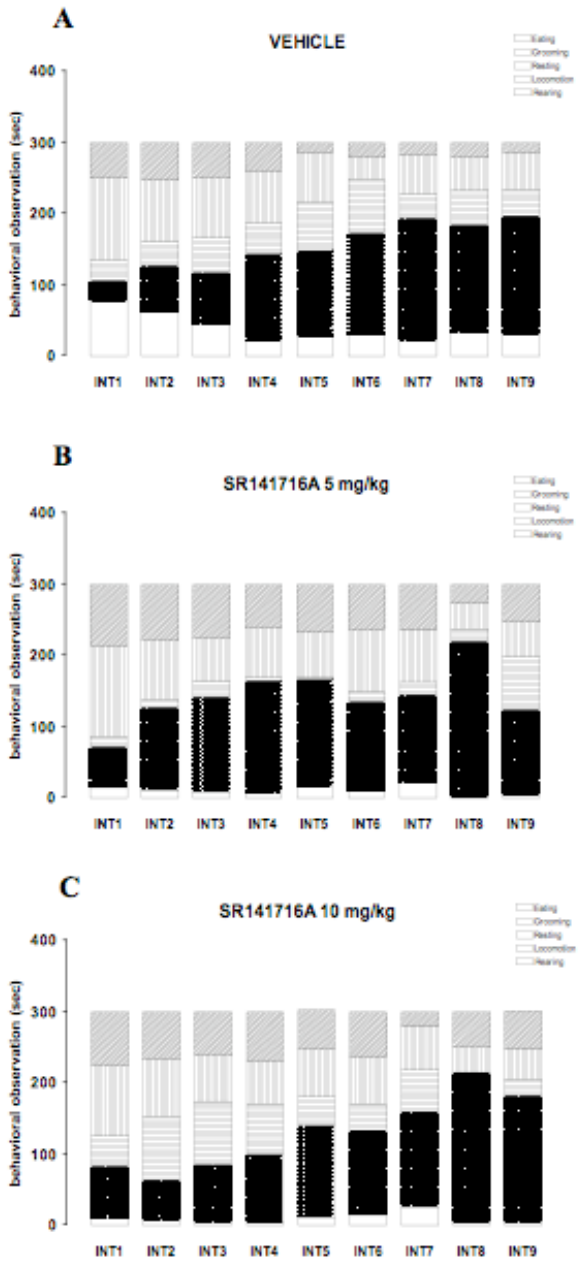

Figure 2. Temporal trend of eating, grooming, resting, locomotion and rearing duration. Panels show the results for vehicle group (A), SR171416A (5 mg/kg) (B) and SR171416A (10 mg/kg) (C) administered mice. Represented on the X-axes are 9 time bins of 5 min each for a total 45 min of behavioral observation.

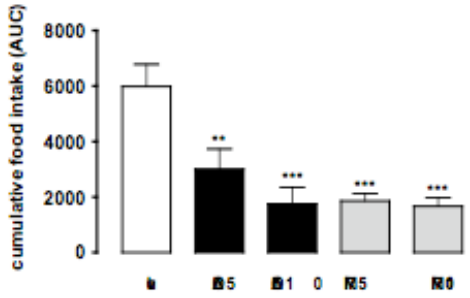

Figure 3. Cumulative food intake of eating affected by drug treatment.